Graduate Theses and Dissertations   Graduate School

11-17-2015

Molecular and Phenotypic Studies Validating the Role of the Ecdysone Receptor in the Human Parasite *Brugia malayi*

Amruta Mhashilkar
University of South Florida, amhashil@health.usf.edu

Molecular and Phenotypic Studies Validating the Role of the Ecdysone Receptor in the

Human Parasite *Brugia malayi*

by

Amruta S. Mhashilkar

A dissertation submitted in partial fulfillment
of the requirements for the degree of
Doctor of Philosophy
Department of Global Health
College of Public Health
University of South Florida

Major Professor: Thomas R. Unnasch, Ph.D.
Dennis Kyle, Ph.D.
Bill Baker, Ph.D.
Rays Jiang, Ph.D.

Date of Approval:
November 13, 2015

Keywords: Lymphatic filariasis, RNA-seq, transcriptomics, proteomics, homology
modeling, drug discovery

DEDICATION

I want to dedicate my dissertation to my parents, Mrs. Vasanti Mhashilkar and Mr. Sudhakar Mhashilkar. Thank you for believing in my dreams and supporting my decision to pursue higher studies in the United States. You have made me the person I am today. More importantly, I am thankful for every effort you have taken for me. I could not have done this without your support and encouragement. I would like to thank my husband, Mahtab Shaikh for the constant positive reassurance, putting up with all of my craziness and taking care of me during my dissertation process. I owe you so much. I would also like to thank my friends, especially "USF Buddies", Prerna, Pooja and Sushma for the emotional support during my doctoral studies. A special thanks to Andrea for being there for me during my highs and lows throughout my doctoral studies. I don't know what I would have done without you. I would also like to thank my committee for providing valuable support during the process. Lastly, I want to thank my mentor Dr. Thomas Unnasch for believing me with the project, inspiring me to achieve the best and provide more than valuable wisdom.

TABLE OF CONTENTS

LIST OF TABLES

iii

LIST OF FIGURES

ABSTRACT

Filariasis and onchocerciasis are debilitating diseases affecting 120 million people globally. The massive socio-economic impact of these diseases energized the international community to declare a goal of eliminating filariasis 2020. This resulted in a dramatic increase in the efforts to eliminate filariasis and onchocerciasis, employing a strategy of mass drug administration (MDA). However, these programs rely upon the small arsenal of drugs. This leaves these programs vulnerable to failure in the face of developing resistance and local intolerance to the current drug regimens. Thus, new drugs against these infections are critically needed. A homologue of the ecdysone receptor (EcR), a master regulator of development in insects, has been identified in *B. malayi*. The potential of the EcR as a drug target has been underscored by work in the agricultural industry, where insecticides targeting the ecdysone developmental pathway are effective and non-toxic to non-target species. As the EcR is absent in humans, it represents an attractive potential chemotherapeutic target. The first study investigates the hypothesis that the ecdysone receptor controls the embryogenesis and molting in the filarial parasite. *In-vitro* embryogram and *in-vivo* phenotypic studies were conducted to delineate the effect of 20-hydroxyecdysone on the *Brugia malayi* parasites. The results suggest that the hormone accelerates embryogenesis and causes precocious molts, resulting in the death of the parasite. Further, transcriptomic and proteomic analysis of the ecdysone treated worms provided evidence that the up-regulated genes

participate in embryogenesis. Based upon the validation of the ecdysone receptor as a potential drug target, subsequent studies focused on the development of a drug discovery model to screen for agonists and antagonists of the *B. malayi* ecdysone receptor. A stable cell line was created to aid the high throughput screening to rapidly identity agonist and antagonist compounds. A total of 7 agonists and 2 antagonists were identified. A homology model of the *Bm*EcR ligand-binding domain was created as an alternate method for virtual screening of small molecules as well as to study the ligand-receptor interactions. The hits identified with the assay were docked in the active site of the *Bm*EcR homology model providing an excellent correspondence of data between the molecular assay and the virtual screening method.

CHAPTER ONE

INTRODUCTION

Current Scenario of the Parasitic Nematodes

The phylum nematoda consists of round worms with more than 25,000 species described. Members of this phylum can be free-living or parasitic in nature [1, 2]. A large number of these species are parasites of humans. Over 2 billion people in developing countries harbor more than one species of parasitic nematode [3]. Filarial nematodes and soil-transmitted nematodes pose a serious threat to health of individuals and livestock. *Onchocerca volvulus*, a filarial nematode parasite of humans, causes severe debilitating pathologies that range from dermatitis to vision loss [4]. Gastrointestinal nematodes cause nutritional deficiencies, anemia, growth problems and cognitive deficiencies in school aged children [5, 6]. Apart from the health impacts, parasitic nematodes have caused significant economic losses. *Ascaris suum* infection results in an annual economic loss of $155 million in the US alone [7]. Agricultural loss caused by parasitic nematodes is estimated to total more than $100 billion globally [8].

The overall impact of parasitic nematodes on human health is significant. The

absence of vaccines aggravates the problem. Most of the prevention and control program depend upon chemotherapeutic agents [9]. Anti-helmintic drugs like Ivermectin, benzimidazoles and levimasoles are available, but fall short given the diversity of the parasitic species and the population at risk [10]. More than 1500 new drugs have been introduced in market since 1975, but only two of them (albendazole and ivermectin) have been approved to treat the human nematode infections [11, 12]. Ivermectin and diethylcaramazine (DEC) have been used to treat lymphatic filariasis. These drugs successfully eliminate the microfilariae from the circulation of an infected individual and hence prove to be essential microfilaricidals [13-16]. Drugs that target adults are yet to be identified and the need for a potent macrofilaricide is ever growing.

Intensive use of broad-spectrum anti-helmintics like albendazoles and ivermectin have led to occurrences of drug resistance [17]. Studies have demonstrated development of benzimidazole resistance-associated mutations in the filarial nematode *Wuchereria bancrofti* [18]. Levamisole, a drug targeting the nicotinic acetylcholine receptor was introduced in 1970 and resistance was conformed in 1979 in *Trichostrongylus colubriformis* 10 301 [9, 19]. A detailed understanding of the nematode parasites is essential to develop newer and effective chemotherapeutic agents.

Parasitic nematodes pose a serious public health problem and inflict debilitating lifelong morbidity and mortality in the endemic countries [20]. A better understanding of the parasites biochemistry and physiology is necessary in order to develop new and novel anthelmintic drugs to combat parasitic nematode development.

Overview of the Lymphatic Filariasis (LF)

Filarioidea are a superfamily within the order Spirurida, comprising nematodes that parasitize variety of amphibian to mammalian species. An insect vector plays an important role in the developmental cycle of the filarial worms. Lymphatic Filariasis (LF) is caused by *Wuchereria bancrofti* (accounting for approximately 90% of cases), *Brugia malayi* and *Brugia timori* [21]. Lymphatic filariasis has been identified as the second leading cause of infection resulting in permanent and long-term disability [22]. It is estimated that more than 1.23 billion people in 58 countries globally are at risk for lymphatic filariasis. More than 120 million people are infected and carrying the burden of the disease. Approximately 40 million people live with disability and deformity affecting their livelihood[3, 23]. As a result, the World Health Assembly's International Task Force has identified LF as one of six Neglected Tropical diseases targeted for elimination [24].

Pathogenesis

The normal lymphatic vessels arise in the upper dermis channeling through lymphatic vessels draining directly into the lymph nodes [25]. In lymphatic filariasis, the lymphatic channels are dilated and the flow of lymph is compromised. The peripheral lymphatic system is overloaded by the demands of the venous supply. Hence, severe edema of skin and subcutaneous tissue is observed [25, 26]. The damage to the lymphatic vessels occurs due to mechanical trauma cause by microfilariae [27, 28]. The larva triggers a host immune response leading to phagocytosis and microfilarial degeneration [28-33]. The immune responses further stimulate lymphatic vessel dilation. *Wolbachia*, an endosymbiont of the parasite also elicits immune responses

contributing to the lymphatic vessel injury [34].

Lymphatic filariasis display variety of clinical symptoms, that range from being asymptomatic case to a fulminant inflammatory and edematous condition [35]. The upright human posture leads to collection of lymph in the legs. A normal healthy lymphatic system is capable of draining the vessels. But, in LF, a chronic lymphatic failure leads to limb immobility in the dependent position [25]. Extravasation and accumulation of fluid in the tissue leads to edema generally in the legs and genitilia, which is also less commonly observed in the breast tissue and arms [26].

Life cycle of the *Brugia malayi*

The human filarial parasites require a mosquito intermediate host for development while propagating through human and a few other mammalian definitive hosts [36]. The mosquitoes of genera *Mansonia, Aedes, Anopleles* and *Culex* serve as natural vectors for lymphatic filariasis [37]. Mosquitoes bite an infected host and ingest circulating microfilariae during blood meal as seen in Figure 1. Inside the mosquito, the microfilariae sense a temperature and environmental change [38-41]. They penetrate and gain access to hemocoel within a few hours of ingestion [25]. They migrate through the hemolymph to the thoracic musculature [37, 42]. They harbor in the flight muscles and develop into non-feeding sausage-shaped L1 larvae. The parasite molts from L1 to L2 in the flight muscles. The L2 stage larva quickly elongates and increases several times in length by feeding on the mosquito cellular components. The L2 stage larva molt into L3 infective stage larva [43]. Overall, the larva grows from ~200 µm to fully grown

infective stage larva (L3) ~1350 μm within the mosquito in a span of 10-12 days [42].

The L3 stage larva migrate to the proboscis of the mosquito until the mosquito takes its

next blood meal 56 [37]. When the mosquito bites a new mammalian host, the L3 larva

exits the labellum of the mosquito proboscis into the host skin.

In the new mammalian host, the infectious L3s migrate to the lymphatic vessels

where they undergo two additional molts transforming into L4s and finally adults [37].

The adults mature into male and female worms in approximately a year. The adults can

live in the lymphatic system for 10-15 years. The female worm matures and begins

mating, producing large number of microfilariae. The microfilariae enter the blood

stream and are picked up by a new mosquito [44], perpetuating the lifecycle.
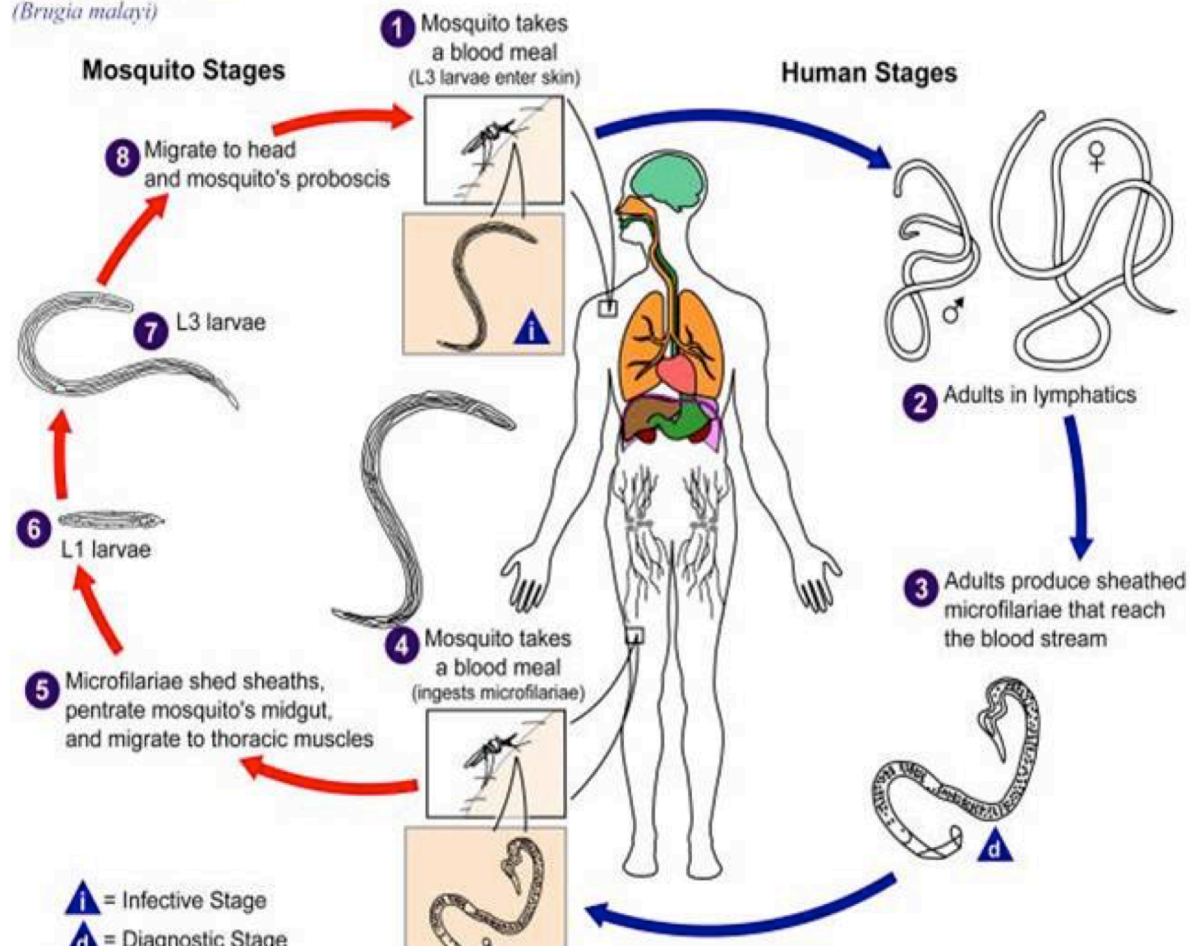
Figure 1.1: The figure *from* Center for Disease Control filariasis webpage showing the life cycle of *Brugia malayi*.[45]

Geographic distribution

Filarial infections are endemic to more than 80 countries in the tropics as shown in figure 1.2. They pose a big problem in South-East Asia, Africa, the Western Pacific and part of the Americas. Around 80 % of the burden of the disease is concentrated in the 10 countries: Bangladesh, Côte d'Ivoire, Democratic Republic of Congo, India, Indonesia, Myanmar, Nigeria, Nepal, Philippines and the United Republic of Tanzania[3].
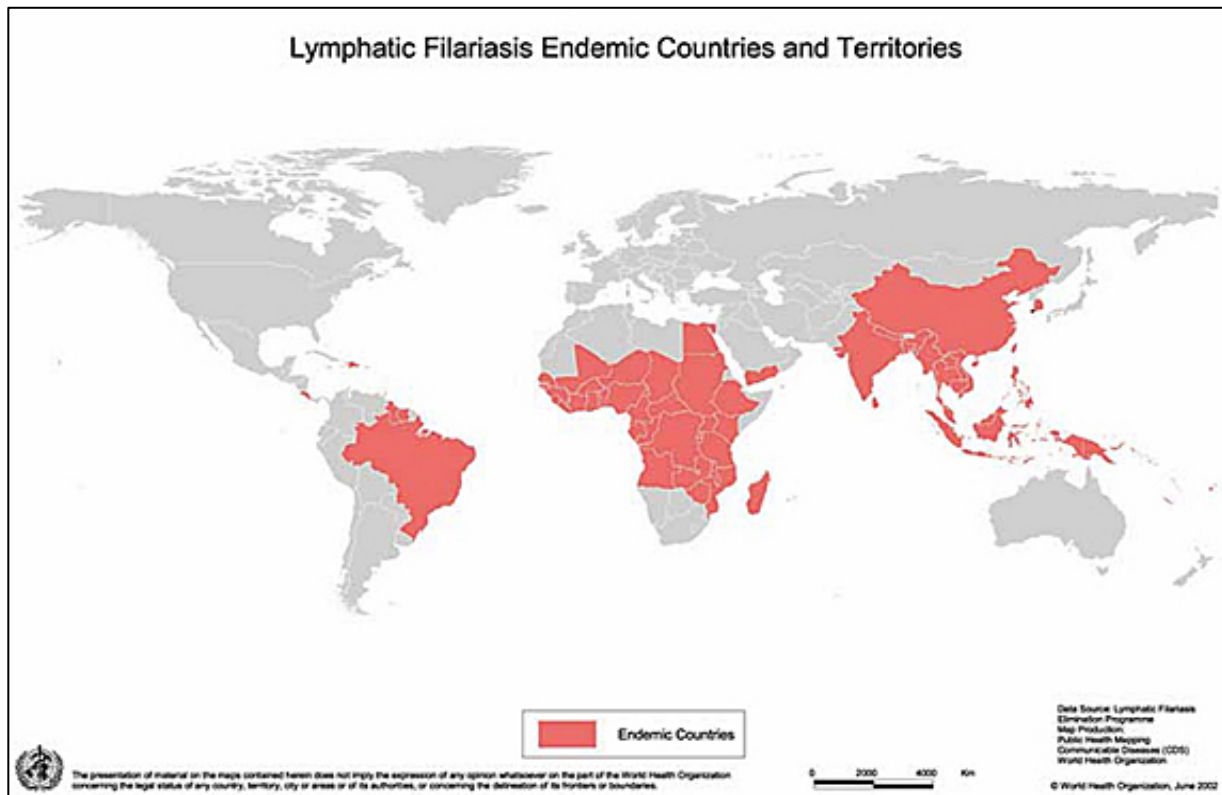
Figure 2: Map from World Health Organization showing lymphatic filariasis endemic countries and territories.[46]

Socioeconomic impact

LF and Onchocerciasis have together resulted in the loss of 5.7 million disability adjusted life years [47]. More than $1 billion in lost productivity each year is observed in India due to lymphatic filariasis whereas another $1 billion for endemic foci in the continent of Africa [48]. A study in rural India of male-weavers afflicted with LF reported a greater than 27.4% productivity loss [49]. Apart from the economic burden, an individual affected with LF faces social stigma, psychological problems, fear and embarrassment [50]. Often suicidal cases, broken marriages due to lack of physical intimacy are reported [50]. More than 40 million demonstrate deformities leading to social stigma and massive economic loss [3].

Efforts in controlling LF globally

Despite promising research and valid targets, an anti-filarial vaccine is yet to be launched for global use [51-56]. Vector control has been conducted in areas where malarial and filarial infections are co-endemic. These methods prove beneficial for geographically isolated areas. A good example of this would be Solomon Islands. Vector control strategies have reduced the prevalence of filarial infection to less than 2% [57, 58]. Unfortunately, vector control programs are very expensive and labor intensive [57]. Insecticide resistance, adverse reactions to insecticides, lack of infrastructure to conduct the programs still pose a challenges to implement the programs in a third world countries [59]. Chemotherapeutic intervention along with vector control serves as a better strategy and play an integral role in filariasis prevention and control[55, 60].

Global Program for the Elimination of Lymphatic Filariasis (GPELF): success and complications

The Global Program for the Elimination of Lymphatic Filariasis (GPELF) was launched in the year 2000 with an ambitious goal to decrease the incidence and prevalence of lymphatic filariasis and eventually eliminate the disease. During the initial years, approximately 570 million people were at risk of the disease [61]. China and South Korea have eliminated lymphatic filariasis in the year 2007 and 2008, respectively. Out of the total 72 participating countries, 68 countries have completed mapping their endemic foci, 11 countries have made progress and 2 have yet to start the process [3]. The total number of population treated under MDA has increased from 2.9 million in the year 2000 to more than 500 million in the year 2010. A total of 17 countries out of the 53 countries have already completed five or more rounds with 100% of geographical coverage [3].

Despite a huge success of the GPELF program, no convincing evidence has been produced to demonstrate that the ultimate goal to eliminate lymphatic filariasis is achievable [62]. Patient compliance and cooperation from the governments pose significant challenge for success of the GPELF program. Further challenges to the GPELF include natural disasters and political unrest, which force populations to migrate to non-MDA covered zones, disrupting the therapy.

Chemotherapeutic agents

Prior to GPELF, diethylcarbamazine (DEC) was distributed to mass populations

as a 0.1- 0.4% fortified salt [63]. This strategy has been used primarily in China, Taiwan, India and Brazil [64, 65]. DEC is primarily used in LF mono-endemic area [66]. It is contraindicated for its use in areas co-endemic with *Onchocerca volvulus* as it can cause severe ocular and systemic complications in individuals infected with this parasite [67]. Similarly, Ivermectin is contraindicated in areas that show prevalence *Loa loa* infections due to severe and fatal adverse effects in *L. loa* infected individuals [68]. Albendazole is used by the GPELF to replace DEC and ivermectin is areas where these drugs are contra-indicated. [69]. Currently, GPELF is providing mass drug administration programs (MDA) in the endemic countries with donated drugs from GlaxoSmithKline and Merck & Co. Inc. More than 52 nations have adopted the MDA strategy to combat lymphatic filariasis. Depending upon the endemicity of the infection, DEC and Ivermectin are given along with albendazole. Monotherapy with albendazole does not have much effect on the microfilarial load in the blood. When given in conjunction with DEC or IVR, albendazole seems to have a synergistic effect. More than 3.4 billion treatments were delivered to more than 900 million of individuals in 53 countries between 2000- 2010 [3].

Problems with current therapy

The backbone of the current MDA programs is formed by DEC and Ivermectin, the only two drugs approved for human therapy. These drugs are potent microfilaricidal but exhibit little effect on adult worms. Little evidence is available showing the efficacy of DEC against adult worms, with most studies suggesting an maximal effect of killing 40% adult worms. But treatment alone with DEC is insufficient to cure an individual [62,

70, 71]. Ivermectin act on the glutamate gated chloride channels in free-living

nematodes [72]. But in culture, Ivermectin shows little to no effect on microfilariae [16].

The pharmacological basis of microfilaricidal effect of both DEC is yet to be resolved.

Brief Overview of the Ecdysone Receptor

Ecdysteroids

Ecdysteroids (a term first coined by Goodwin and colleagues in 1978[73]) are the

best characterized and most understood insect hormones. The first ecdysone hormone

identified was α-ecdysone (now called ecdysone) and the second was β-ecdysone (now

commonly called 20-hydroxyecdysone)[74]. Ecdysone was the first insect hormone to

be isolated and first appeared in an article in June 1954 [75]. Ecdysteroids were initially

identified as the molting hormones. Later on, much evidence was provided to proving

their involvement in other developmental processes. In some insects, ecdysteroids

induce vitellogenin synthesis that aids formation of oocyte. Ecdysteroids modulate and

choreograph each molt cycle from early embryogenesis through metamorphosis.

Ecdysone is produced by the prothoracic gland and gets converted into 20HE in

peripheral tissues [76]. 20HE is the molecule responsible for controlling apolysis of old

cuticle and deposition of new cuticle in insects [77]. It also stimulates embryological

events in the female insect irrespective to the cuticle synthesis [74]. Ecdysteroids have

found to modulate molting in all the species of insects, whether they undergo complete

metamorphosis (such as moths and flies) or undergo incomplete metamorphosis (such

as locusts) [74]. To date, more than 500 unique ecdysteroids have been identified from

plant and animal sources. 20HE has also been identified in non-arthropod invertebrates

the nematodes, mollusks and annelids [78].

Ecdysone receptor

The ecdysone receptor (EcR) belongs to the nuclear receptor (NHR) super family[79]. All members of the NHR family share similar modular structure with functionally distinct domains[80]. The N-terminal A/B domain followed by the DNA-binding C domain, the hinge D domain and the ligand-binding EF domain at the C-terminal end of the protein as shown in Figure 1.3[80, 81]. The E/F domain is

Figure 1.3: Nuclear receptor structure with distinct domains.
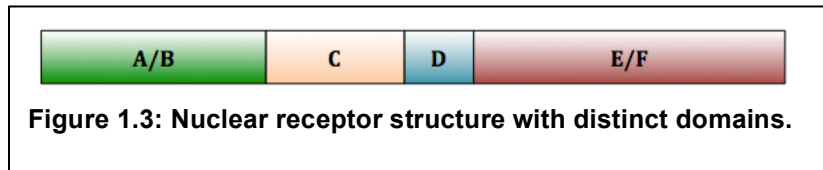
multi-functional, responsible for ligand binding, ligand dependent transactivation and dimerization. The C domain functions as a ligand independent DNA binding domain [81]. This domain dictates the specificity of the response elements. The ecdysone receptor dimerizes with USP (ultraspiracle) or RXR (Retinoic X receptor vertebrate ortholog of USP) and binds with very specific ecdysone receptor response elements (EcREs). The response elements are short DNA sequences, usually 5-20 bp in length, within the promoter of the gene that has the capability of binding their specific hormone receptor and regulate their transcription [82]. In *Drosophila melanogaster* the promoters of several transciptional regulators including E75A, BHR3-B, EcR-B1 contains EcREs that are recognized by the activated EcR [83]. Binding of the EcR to these promoters activates their transcription, leading to activation of many downstream genes, the so called "ecdysone cascade".

The ligand-binding domain of the EcR is the central unit of any ecdysone controlled gene switch. The ligand-binding domain of the ecdysone receptor has two formative characteristics; instability and adaptability of structure. The α-helices 3, 5, 7, 11 and 12 and the β-sheet provide the receptor an apo-conformation, a remarkable capability to bind different types of ligands [84]. Hence, this explains presence of more than 500 ecdysteroids in nature.

Role of ecdysone receptor in insects

Holometabolous insects like *Drosophila melanogaster* undergo a complete metamorphological transformation from a crawling larva to an adult capable of flight and reproduction [85, 86]. This developmental pathway is controlled by a balance of the ecdysteroids and juvenile hormones, with the ecdysteroids stimulating and the juvenile hormones repressing molting [87, 88]. There are carefully timed spurts of 20HE release during the larval molts, pupariation, pupation and transformation in adults. The release of 20HE is choreographed by prothoracicotropic hormone, which is produced by four dorsolateral neurosecretory cells of brain [89-91]. Pulses of 20 HE trigger pre-pupal development forming a puparium. The larval midgut and anterior muscles are destroyed in response to 20HE, while the imaginal discs evert to form the rudimentary structures corresponding to the adult fly [88, 92, 93]. Within 10-12 hours, another pulse of 20HE triggers pre-pupal to pupal transformations. Following apoptotic changes, adult head, body, legs and wings emerge.

Ecdysteroids bind to the EcR-USP heterodimer, which then migrates to the nucleus and activates transcription of a cascade of "early genes", "early-late genes",

and "late genes" in an autoregulatory loop [94]. 20HE can bind to the ligand-binding domain on its own, but the binding is greatly stimulated by the presence of USP [89, 95]. The early genes Broad- Complex (BR-C), E74, and E75 also belong to the NHR family, although most of them are orphan receptors. Studies have demonstrated that E75 and BR-C genes are essential for the appropriate development response on stimulus with 20HE[88].

Ecdysone receptor in gene switching

The Ecdysone receptor and ecdysteroids have been known to modulate molting and developmental changes in insects. Their natural absence in vertebrate makes them an excellent target for gene switch applications due to less possibility of pleotropic effects [81, 96]. The theory behind gene switching is that the hormone receptor binds with a short DNA sequence in the promoter region of a gene turning its transcription ON or OFF, depending upon binding of a ligand. The ecdysone receptor has been extensively used as a gene switch to regulate expression of key genes that regulate molting and metamorphosis. Studies have shown an ecdysone inducible gene expression of the EcR of *Drosophila melanogaster* in a mammalian cell line [97]. Non-steroidal agonists come into play as ligands for the gene switch machinery. Diacylhydrazines were the first discovered non-steroidal ecdysone receptor analogs in 1988[78]. Invitrogen marketed the first commercial ecdysone based gene switch. A fusion protein of VP16 with *Drosophila* ECR LBD with a CMV promoter and a complete human RXR with a RBS promoter were created. The reporter gene was cloned under the control of heat shock protein (HSP) minimal promoter and 5XE/GRE and 3X SP1

response elements. The plasmids were transfected in a RXR deficient cell line and treated with Ponasterone A to induce the system. A successful gene switch was created ready to identify ligands binding with the active site of EcRLBD[81]. Tebufenozide was one of the first non-steroidal compounds that gave high transactivation of the reporter genes through *Bombyx mori* EcR [98, 99]. To improve the functionality of the ecdysone based gene switch, a two-hybrid format of gene switch was formulated. The GAL4 DBD fused with EcR LBD and VP16 fused with RXR constructs under the control of SV40 promoter with firefly luciferase promoter gene was transfected in a EXR deficient cell line[100]. This system has been extensively used for ecdysone based gene switches.

The first successful use of ecdysone analog for insect control was reported in 1980s with the discovery of diacylhydrazines. This class of compounds induces precocious molting of larva in susceptible species [101]. The narrow window of activity against a specific pest species makes it an excellent tool for pest management. Tebufenozide has insecticidal activity against lepidopteran pests but shows no activity against the hymenopteran insects. Tebufenozide, Methoxyfenozide, Halofenozide and Chromafenozide are the four commercially available insecticides for lepidopteran and coleopteran control [81]. In a bioassay, the tetrahydroquinolone family have shown high activity against *A. aegypti* [102].

Transgenic plants have also been produced using the gene switch technology. The first ecdysone based gene switch was developed in 1999 [81, 103]. Transgenic tabacco plants were created that were dependant on tebufenozide induced expression of a reporter gene regulated by this EcR-based gene switch [103]. However, the

continuous need of a ligand to activate the gene switch and background activity of the gene switch limited the use of this technology in the agricultural industry.

Ecdysone Receptor in Nematodes

Nematodes are theorized to be ecdysozoans due to primacy of molting in their development. Homologues of the EcR and analogs many of the downstream genes activated by the EcR have been identified in the filarial parasites [104]. Surprisingly, the ecdysone receptor and its dimerizing partner RXR are absent in *C.elegans* [104]. Molting in *C.elegans* is controlled by a different set of nuclear receptors including NHR-25, 41, 67. These coincide with the homologs of the downstream genes activated in the insects [104]. However, control of molting in the filaria remains a relatively unknown topic, and the genes participating in the molting cascade are yet to be identified. Low concentrations of ecdysteroids have induced molting of *Nematospiroides* dubius [105] and *Ascaris suum* [106]. Successful artificial molting has been also been induced with ecdysone analogs including 20HE and RH5849 in *D.immitis* culture [107-109]. In some nematodes such as with *Meloidogyne javanica*, 20HE has caused mortality of the organism without inducing any morphological or molting changes [110, 111]. High molar concentrations (4.2 to 8.4mM) of 20HE have reported to inhibit development from eggs to larval stages and death of the *H. contortus* within a week [110].

Brugia malayi Ecdysone Receptor

The ecdysone receptor and the RXR homologs have been identified in the *B. malayi* and *O. volvulus* [104]. The ecdysone receptor is expressed in *B. malayi* in L1,

L2, L3, adult males and females, while the *B. malayi* RXR homologe is expressed predominantly in L1, adult males and females [109]. *Brugia malayi* EcR, when partnered with the *Aedes aegypti* USP (AaUSP) displayed binding with a synthetic palindromic ecdysone response element (EcRE), PAL-1[104]. The protein encoding the ecdysone receptor is shown to dimerize with native *Brugia* RXR as well as RXR from other organisms. This indicates the ecdysone receptor of *Brugia malayi* exhibits behavior similar to the insect EcRs. Furthrmore, an ecdysone response element (EcRE) inserted in a synthetic *Brugia malayi* promoter was induced by 20HE in transiently transfected *Brugia* embryos [109]. Together, these studies suggest an existence of a functional ecdysone-signaling pathway in the B. *malayi*.

Objective

Previous research provides substantial evidence of a functional ecdysone signaling system in *Brugia malayi*. Yet, the role played by ecdysone on embryogenesis and molting is unclear. This research attempts to further investigate the physiological role and chemotherapeutic potential of the ecdysone receptor in *Brugia malayi*. The first part of the study aims on examining phenotypic and biochemical changes on adult female worms in presence of 20HE. Transcriptomic and proteomic studies were performed to observe differential gene expression in the treated adult female worms. The second part of the study focused on the phenotypic study conducted *in-vivo* and the chemotherapeutic potential of the *Brugia* ecdysone receptor. A homology model of the EcR was developed to provide insights about the ligand-receptor interaction.

References

1.   Zhang, Z.-Q., *Animal biodiversity: An update of classification and diversity in 2013. In : Zhang, Z.-Q. (Ed.) Animal Biodiversity: An Outline of Higher-level Classification and Survey of Taxonomic Richness (Addenda 2013).* 2013, 2013. **3703**(1): p. 7.

2.   Zhang, Z.-Q., *Phylum Nematoda Cobb, 1932. In : Zhang, Z.-Q. (Ed.) Animal Biodiversity: An Outline of Higher-level Classification and Survey of Taxonomic Richness (Addenda 2013).* 2013, 2013. **3148**: p. 63.

3.   Who, *Lymphatic filariasis.* 2000, World Health Organization: Geneva.

4.   Lustigman, S., et al., *RNA interference targeting cathepsin L and Z-like cysteine proteases of Onchocerca volvulus confirmed their essential function during L3 molting.* Molecular and Biochemical Parasitology, 2004. **138**(2): p. 165-70.

5.   Bethony, J., et al., *Soil-transmitted helminth infections: ascariasis, trichuriasis, and hookworm.* Lancet, 2006. **367**(9521): p. 1521-32.

6.   Crompton, D.W. and M.C. Nesheim, *Nutritional impact of intestinal helminthiasis during the human life cycle.* Annu Rev Nutr, 2002. **22**: p. 35-59.

7.   Martin, R.J., et al., *Oxantel is an N-type (methyridine and nicotine) agonist not an L-type (levamisole and pyrantel) agonist: classification of cholinergic anthelmintics in Ascaris.* Int J Parasitol, 2004. **34**(9): p. 1083-90.

8.   Li, J., et al., *Biotechnological application of functional genomics towards plant-parasitic nematode control.* Plant Biotechnol J, 2011. **9**(9): p. 936-44.

9.   James, C.E., A.L. Hudson, and M.W. Davey, *Drug resistance mechanisms in helminths: is it survival of the fittest?* Trends Parasitol, 2009. **25**(7): p. 328-35.

10.   Doenhoff, M.J., D. Cioli, and J. Utzinger, *Praziquantel: mechanisms of action, resistance and new derivatives for schistosomiasis.* Curr Opin Infect Dis, 2008. **21**(6): p. 659-67.

11.   Chirac, P. and E. Torreele, *Global framework on essential health R&D.* Lancet, 2006. **367**(9522): p. 1560-1.

12.   Stern, E.J., *Forgotten People, Forgotten Diseases: The Neglected Tropical Diseases and Their Impact on Global Health and Development. 2d ed.* Clinical Infectious Diseases, 2013. **57**(12): p. 1793-1794.

13.   Ottesen, E.A., et al., *The Global Programme to Eliminate Lymphatic Filariasis: Health Impact after 8 Years.* PLoS Negl Trop Dis, 2008. **2**(10): p. e317.

14.   Bennett, J.L., J.F. Williams, and V. Dave, *Pharmacology of ivermectin.* Parasitology Today, 1988. **4**(8): p. 226-228.

15.   Noroes, J., et al., *Assessment of the efficacy of diethylcarbamazine on adult Wuchereria bancrofti in vivo.* Trans R Soc Trop Med Hyg, 1997. **91**(1): p. 78-81.

16.   Pax, R.A., J.F. Williams, and R.H. Guderian, *In vitro motility of isolated adults and segments of Onchocerca volvulus, Brugia pahangi and Acanthocheilonema viteae.* Trop Med Parasitol, 1988. **39 Suppl 4**: p. 450-5.

17.   Mccarthy, J., *Is Anthelmintic Resistance a Threat to The Program to Eliminate Lymphatic Filariasis?* The American Journal of Tropical Medicine and Hygiene, 2005. **73**(2): p. 232-233.

18.   Schwab, A.E., et al., *Detection of Benzimidazole Resistance–Associated Mutations in the Filarial Nematode Wuchereria Bancrofti and Evidence for Selection by Albendazole and Ivermectin Combination Treatment.* The American Journal of Tropical Medicine and Hygiene, 2005. **73**(2): p. 234-238.

19.   Sangster, N.C., et al., *Trichostrongylus colubriformis and Ostertagia circumcincta resistant to levamisole, morantel tartrate and thiabendazole: occurrence of field strains.* Res Vet Sci, 1979. **27**(1): p. 106-10.

20.   Colley, D.G., *Parasitic diseases: opportunities and challenges in the 21st century.* Memórias do Instituto Oswaldo Cruz, 2000. **95**: p. 79-87.

21.   Ottesen, E.A., *The Wellcome Trust Lecture. Infection and disease in lymphatic filariasis: an immunological perspective.* Parasitology, 1992. **104 Suppl**: p. S71-9.

22.   Organization, W.H., *Global programme to eliminate lymphatic filariasis.* Weekly Epidemiological Record, 2009. **42**: p. 437-444.

23.   *TDR News*. 1994, World Health Organization: Geneva.

24.   Molyneux, D.H., et al., *Lymphatic filariasis: setting the scene for elimination.* Trans R Soc Trop Med Hyg, 2000. **94**(6): p. 589-91.

25.   Vaqas, B. and T.J. Ryan, *Lymphoedema: Pathophysiology and management in resource-poor settings - relevance for lymphatic filariasis control programmes.* Filaria Journal, 2003. **2**: p. 4-4.

26.   Shenoy, R.K., *Clinical and Pathological Aspects of Filarial Lymphedema and Its Management.* The Korean Journal of Parasitology, 2008. **46**(3): p. 119-125.

27. Brattig, N.W., et al., *The major surface protein of Wolbachia endosymbionts in filarial nematodes elicits immune responses through TLR2 and TLR4.* J Immunol., 2004. **173**(1): p. 437-45.

28. Hise, A.G., et al., *Innate immune responses to endosymbiotic Wolbachia bacteria in Brugia malayi and Onchocerca volvulus are dependent on TLR2, TLR6, MyD88, and Mal, but not TLR4, TRIF, or TRAM.* J Immunol, 2007. **178**(2): p. 1068-76.

29. Olszewski, W.L., et al., *Bacteriologic studies of skin, tissue fluid, lymph, and lymph nodes in patients with filarial lymphedema.* Am J Trop Med Hyg, 1997. **57**(1): p. 7-15.

30. Freedman, D.O., et al., *Lymphoscintigraphic analysis of lymphatic abnormalities in symptomatic and asymptomatic human filariasis.* J Infect Dis, 1994. **170**(4): p. 927-33.

31. Brattig, N.W., et al., *The major surface protein of Wolbachia endosymbionts in filarial nematodes elicits immune responses through TLR2 and TLR4.* J Immunol, 2004. **173**(1): p. 437-45.

32. Hise, A.G., I. Gillette-Ferguson, and E. Pearlman, *Immunopathogenesis of Onchocerca volvulus keratitis (river blindness): a novel role for TLR4 and endosymbiotic Wolbachia bacteria.* J Endotoxin Res., 2003. **9**(6): p. 390-4.

33. Tesh, R.B. and H. Guzman, *Mortality and infertility in adult mosquitoes after the ingestion of blood containing ivermectin.* Am J Trop Med Hyg, 1990. **43**(3): p. 229-33.

34. Debrah, A.Y., et al., *Doxycycline reduces plasma VEGF-C/sVEGFR-3 and improves pathology in lymphatic filariasis.* PLoS Pathog, 2006. **2**(9): p. e92.

35. Babu, S. and T.B. Nutman, *Immunopathogenesis of lymphatic filarial disease.* Seminars in immunopathology, 2012. **34**(6): p. 847-861.

36. Amaya, K., *Brugia malayi.* (On-line), Animal Diversity Web., 2003.

37. Bartholomay, L.C. and B.M. Christensen, *Vector-Parasite Interactions in Mosquito-Borne Filariasis*, in *The Filaria*. 2002, Springer US. p. 9-19.

38. Hunter, S.J., et al., *Temperature is a cue for gene expression in the post-infective L3 of the parasitic nematode Brugia pahangi.* Mol Biochem Parasitol, 2001. **112**(1): p. 1-9.

39. Thompson, F.J., et al., *Heat shock and developmental expression of hsp83 in the filarial nematode Brugia pahangi.* Eur J Biochem, 2001. **268**(22): p. 5808-15.

40. Devaney, E. and E. Lewis, *Temperature-induced refractoriness of Aedes aegypti mosquitoes to infection with the filaria Brugia pahangi.* Med Vet Entomol, 1993. **7**(3): p. 297-8.

41. Fang, J. and T.F. McCutchan, *Thermoregulation in a parasite's life cycle.* Nature, 2002. **418**(6899): p. 742.

42. Erickson, S.M., et al., *Mosquito infection responses to developing filarial worms.* PLoS Negl Trop Dis, 2009. **3**(10): p. e529.

43. Beckett, E.B., *Histological changes in mosquito flight muscle fibres associated with parasitization by filarial larvae.* Parasitology, 1971. **63**(3): p. 365-72.

44. Devaney, E. and J. Osborne, *The third-stage larva (L3) of Brugia: its role in immune modulation and protective immunity.* Microbes Infect, 2000. **2**(11): p. 1363-71.

45. CDC. *Life Cycle of Brugia malayi.* 2015 March 25, 2015 [cited 2015 10/28/2015]; Available from: http://www.cdc.gov/parasites/lymphaticfilariasis/biology_b_malayi.html.

46. WHO, *The Global Programme to Eliminate Lymphatic Filariasis Annual Report* A. Haden, Editor. 2001, World Health Organization: Geneva.

47. Mathers, C.D., M. Ezzati, and A.D. Lopez, *Measuring the burden of neglected tropical diseases: the global burden of disease framework.* PLoS Negl Trop Dis, 2007. **1**(2): p. e114.

48. Chu, B.K., et al., *The economic benefits resulting from the first 8 years of the Global Programme to Eliminate Lymphatic Filariasis (2000-2007).* PLoS Negl Trop Dis, 2010. **4**(6): p. e708.

49. Samarasinghe, B., D.P. Knox, and C. Britton, *Factors affecting susceptibility to RNA interference in Haemonchus contortus and in vivo silencing of an H11 aminopeptidase gene.* Int J Parasitol, 2011. **41**(1): p. 51-9.

50. Dreyer, G., et al., *Amicrofilaraemic carriers of adult Wuchereria bancrofti.* Trans R Soc Trop Med Hyg, 1996. **90**(3): p. 288-9.

51. Ramu, K., et al., *Impact of lymphatic filariasis on the productivity of male weavers in a south Indian village.* Trans R Soc Trop Med Hyg, 1996. **90**(6): p. 669-70.

52. Taylor, M.J., H.F. Cross, and K. Bilo, *Inflammatory responses induced by the filarial nematode Brugia malayi are mediated by lipopolysaccharide-like activity from endosymbiotic Wolbachia bacteria.* J Exp Med, 2000. **191**(8): p. 1429-36.

53. Chenthamarakshan, V., M.V. Reddy, and B.C. Harinath, *Immunoprophylactic potential of a 120 kDa Brugia malayi adult antigen fraction, BmA-2, in lymphatic filariasis.* Parasite Immunol, 1995. **17**(6): p. 277-85.

54. Dissanayake, S., et al., *Differential recognition of microfilarial chitinase, a transmission-blocking vaccine candidate antigen, by sera from patients with Brugian and Bancroftian filariasis.* Am J Trop Med Hyg, 1995. **53**(3): p. 289-94.

55. Grieve, R.B., et al., *Vaccine research and development for the prevention of filarial nematode infections.* Pharm Biotechnol, 1995. **6**: p. 737-68.

56. McCarthy, J.S. and T.B. Nutman, *Perspective: prospects for development of vaccines against human helminth infections.* J Infect Dis, 1996. **174**(6): p. 1384-90.

57. Organization, W.H., *Report on the mid-term assessment of microfilaraemia reduction in sentinel sites of 13 countries of the Global Programme to Eliminate Lymphatic Filariasis.* Weekly Epidemiological Record, 2004. **79**: p. 358-365.

58. Babayan, S.A., J.E. Allen, and D.W. Taylor, *Future prospects and challenges of vaccines against filariasis.* Parasite Immunology, 2012. **34**(5): p. 243-53.

59. Melrose, W.D., *Lymphatic filariasis: new insights into an old disease.* Int J Parasitol, 2002. **32**(8): p. 947-60.

60. Bockarie, M.J., M.J. Taylor, and J.O. Gyapong, *Current practices in the management of lymphatic filariasis.* Expert Rev Anti Infect Ther, 2009. **7**(5): p. 595-605.

61. Hooper, P.J., et al., *The Global Programme to Eliminate Lymphatic Filariasis: health impact during its first 8 years (2000-2007).* Ann Trop Med Parasitol, 2009. **103 Suppl 1**: p. S17-21.

62. Kazura, J.W., *Lymphatic Filarial Infections: An Introduction to the Filariae*, in *THE FILARIA*. 2002, Kluwer Academic Publishers: Massachusettes,. p. 1-8.

63. Meyrowitsch, D.W., P.E. Simonsen, and P. Magnussen, *Tolerance to diethylcarbamazine-medicated salt in individuals infected with Onchocerca volvulus.* Trans R Soc Trop Med Hyg, 2000. **94**(4): p. 444-8.

64. Adinarayanan, S., et al., *Diethylcarbamazine (DEC)-medicated salt for community-based control of lymphatic filariasis.* Cochrane Database Syst Rev, 2007(1): p. Cd003758.

65. Gelband, H., *Diethylcarbamazine salt in the control of lymphatic filariasis.* Am J Trop Med Hyg, 1994. **50**(6): p. 655-62.

66. Satti, M.Z., et al., *Comparative effects of anthelmintics on motility in vitro of Onchocerca gutturosa, Brugia pahangi and Acanthocheilonema viteae.* Trop Med Parasitol, 1988. **39 Suppl 4**: p. 480-3.

67. Awadzi, K., *Clinical picture and outcome of Serious Adverse Events in the treatment of Onchocerciasis.* Filaria J, 2003. **2**(Suppl 1): p. S6.

68. Twum-Danso, N.A., *Serious adverse events following treatment with ivermectin for onchocerciasis control: a review of reported cases.* Filaria Journal, 2003. **2**(Suppl 1): p. S3.

69. *Global programme to eliminate lymphatic filariasis.* Wkly Epidemiol Rec, 2009. **84**(42): p. 437-44.

70. Dreyer, G., et al., *Direct assessment in vivo of the efficacy of combined single-dose ivermectin and diethylcarbamazine against adult Wuchereria bancrofti.* Trans R Soc Trop Med Hyg, 1998. **92**(2): p. 219-22.

71. Freedman, D.O., et al., *Effect of aggressive prolonged diethylcarbamazine therapy on circulating antigen levels in bancroftian filariasis.* Trop Med Int Health, 2001. **6**(1): p. 37-41.

72. Geary, T.G., et al., *Unresolved issues in anthelmintic pharmacology for helminthiases of humans.* Int J Parasitol, 2010. **40**(1): p. 1-13.

73. Goodwin, T.W., et al., *Ecdysteroids: a new generic term.* Nature, 1978. **272**(5649): p. 122-122.

74. Yund, M.A., *Ecdysteroid Action in Imaginai Discs of Drosophila Melanogaster*, in *Development of Responsiveness to Steroid Hormones*, A.M.K. Kaye, Editor. 1980, Pergamon. p. 285-302.

75. Karlson, P., *On the hormonal control of insect metamorphosis. A historical review.* Int J Dev Biol, 1996. **40**(1): p. 93-6.

76. King, D.S., et al., *The Secretion of alpha-Ecdysone by the Prothoracic Glands of Manduca sexta In Vitro.* Proc Natl Acad Sci U S A, 1974. **71**(3): p. 793-6.

77. Pound, J.M., J.H. Oliver, Jr., and R.H. Andrews, *Induction of apolysis and cuticle formation in female Ornithodoros parkeri (Acari: Argasidae) by hemocoelic injections of beta-ecdysone.* J Med Entomol, 1984. **21**(5): p. 612-4.

78.   Yoshio Takei, H.A., Kazuyoshi Tsutsui, *Handbook of Hormones: Comparative Endocrinology for Basic and Clinical Research*. 2015: Elsevier Science & Technology 674.

79.   Mangelsdorf, D.J. and R.M. Evans, *The RXR heterodimers and orphan receptors.* Cell, 1995. **83**(6): p. 841-50.

80.   Huss, J.M. and D.P. Kelly, *Nuclear Receptor Signaling and Cardiac Energetics.* Circulation Research, 2004. **95**(6): p. 568-578.

81.   Palli, S.R., et al., *Ecdysteroid receptors and their applications in agriculture and medicine.* Vitam Horm, 2005. **73**: p. 59-100.

82.   *Response Element (Molecular Biology).* [cited 2015 October 23]; Available from: http://what-when-how.com/molecular-biology/response-element-molecular-biology/.

83.   Thummel, C.S., *The Drosophila E74 promoter contains essential sequences downstream from the start site of transcription.* Genes Dev, 1989. **3**(6): p. 782-92.

84.   Iwema, T., et al., *Structural and functional characterization of a novel type of ligand-independent RXR-USP receptor.* The EMBO Journal, 2007. **26**(16): p. 3770-3782.

85.   Brody, T., *The Interactive Fly: gene networks, development and the Internet.* Trends Genet, 1999. **15**(8): p. 333-4.

86.   Ureña, E., et al., *Transcription factor E93 specifies adult metamorphosis in hemimetabolous and holometabolous insects.* Proceedings of the National Academy of Sciences of the United States of America, 2014. **111**(19): p. 7024-7029.

87.   Riddiford, L.M., et al., *A role for juvenile hormone in the prepupal development of Drosophila melanogaster.* Development, 2010. **137**(7): p. 1117-26.

88.   Lam, G., et al., *DHR3 is required for the prepupal-pupal transition and differentiation of adult structures during Drosophila metamorphosis.* Dev Biol, 1999. **212**(1): p. 204-16.

89.   Dai, J.D. and L.I. Gilbert, *Metamorphosis of the corpus allatum and degeneration of the prothoracic glands during the larval-pupal-adult transformation of Drosophila melanogaster: a cytophysiological analysis of the ring gland.* Dev Biol, 1991. **144**(2): p. 309-26.

90.   Caldwell, P.E., M. Walkiewicz, and M. Stern, *Ras activity in the Drosophila prothoracic gland regulates body size and developmental rate via ecdysone release.* Curr Biol, 2005. **15**(20): p. 1785-95.

91.   Mansilla, A., et al., *Ligand-independent requirements of steroid receptors EcR and USP for cell survival.* Cell Death Differ, 2015.

92.   Robertson, C.W., *The metamorphosis of Drosophila melanogaster, including an accurately timed account of the principal morphological changes.* Journal of Morphology, 1936. **59**(2): p. 351-399.

93.   Jiang, C., E.H. Baehrecke, and C.S. Thummel, *Steroid regulated programmed cell death during Drosophila metamorphosis.* Development, 1997. **124**(22): p. 4673-83.

94.   Tata, J.R., *Signalling through nuclear receptors.* Nat Rev Mol Cell Biol, 2002. **3**(9): p. 702-710.

95.   Jakób, M., et al., *Novel DNA-binding element within the C-terminal extension of the nuclear receptor DNA-binding domain.* Nucleic Acids Research, 2007. **35**(8): p. 2705-2718.

96.   Feil, R., et al., *Ligand-activated site-specific recombination in mice.* Proc Natl Acad Sci U S A, 1996. **93**(20): p. 10887-90.

97.   No, D., T.P. Yao, and R.M. Evans, *Ecdysone-inducible gene expression in mammalian cells and transgenic mice.* Proc Natl Acad Sci U S A, 1996. **93**(8): p. 3346-51.

98.   Hoppe, U.C., E. Marban, and D.C. Johns, *Adenovirus-mediated inducible gene expression in vivo by a hybrid ecdysone receptor.* Mol Ther, 2000. **1**(2): p. 159-64.

99.   Swevers, L., et al., *The silkmoth homolog of the Drosophila ecdysone receptor (B1 isoform): cloning and analysis of expression during follicular cell differentiation.* Insect Biochem Mol Biol, 1995. **25**(7): p. 857-66.

100.   Palli, S.R., et al., *Improved ecdysone receptor-based inducible gene regulation system.* Eur J Biochem, 2003. **270**(6): p. 1308-15.

101.   Dhadialla, T.S., G.R. Carlson, and D.P. Le, *New insecticides with ecdysteroidal and juvenile hormone activity.* Annu Rev Entomol, 1998. **43**: p. 545-69.

102.   Palli, S.R., et al., *Biochemical mode of action and differential activity of new ecdysone agonists against mosquitoes and moths.* Arch Insect Biochem Physiol, 2005. **58**(4): p. 234-42.

103. Martinez, A., et al., *Ecdysone agonist inducible transcription in transgenic tobacco plants.* Plant J, 1999. **19**(1): p. 97-106.

104. Tzertzinis, G., et al., *Molecular evidence for a functional ecdysone signaling system in Brugia malayi.* PLoS Negl Trop Dis, 2010. **4**(3): p. e625.

105. Dennis, R.D., *Insect morphogenetic hormones and developmental mechanisms in the nematode, Nematospiroides dubius.* Comp Biochem Physiol A Comp Physiol, 1976. **53**(1): p. 53-6.

106. Fleming, M.W., *Ascaris suum: role of ecdysteroids in molting.* Exp Parasitol, 1985. **60**(2): p. 207-10.

107. Barker, G.C. and H.H. Rees, *Ecdysteroids in nematodes.* Parasitol Today, 1990. **6**(12): p. 384-7.

108. Warbrick, E.V., et al., *The effect of invertebrate hormones and potential hormone inhibitors on the third larval moult of the filarial nematode, Dirofilaria immitis, in vitro.* Parasitology, 1993. **107 (Pt 4)**: p. 459-63.

109. Liu, C., et al., *Identification of genes containing ecdysone response elements in the genome of Brugia malayi.* Molecular and biochemical parasitology, 2012. **186**(1): p. 38-43.

110. Graham, L.D., et al., *An ortholog of the ecdysone receptor protein (EcR) from the parasitic nematode Haemonchus contortus.* Mol Biochem Parasitol, 2010. **171**(2): p. 104-7.

111. Soriano, I.R., et al., *Phytoecdysteroids: a novel defense against plant-parasitic nematodes.* J Chem Ecol, 2004. **30**(10): p. 1885-99.

CHAPTER TWO

PHENOTYPIC AND MOLECULAR ANALYSIS OF THE EFFECT OF 20-HYDROXYECDYSONE ON THE HUMAN FILARIAL PARASITE *BRUGIA MALAYI*

Abstract

A homologue of the ecdysone receptor has been identified and shown to be responsive to 20-hydroxyecdysone in *Brugia malayi*. However, the role that this master regulator of insect development plays in filarial nematodes has not been delineated. Gravid adult female *B. malayi* cultured in the presence of 20-hydroxyecdysone produced significantly more microfilariae and abortive immature progeny than control worms, implicating the ecdysone receptor in regulation of microfilarial development. Only one adult female worm was recovered on stimulating the ecdysone receptor of the L3 larvae infected intraperitoneally in an *in-vivo* gerbil model. This deduced that ecdysone receptor causes premature molting leading to the death of the parasite. Transcriptome analyses identified 30 genes whose expression were significantly up-regulated in 20-hydroxyecdysone treated parasites compared to untreated controls. Of these, 18% were identified to be involved in regulating transcription. RNAi phenotype of the *C.elegans* orthologs of the up-regulated genes demonstrated that the 20-hydroxyecdysone exclusively regulated embryological events. A comparative proteomic

analysis revealed 932 proteins to be present in greater amounts in extracts of 20-hydroxyecdysone treated adult females than in extracts prepared from worms cultured in the absence of the hormone. Of the proteins exhibiting a greater than two fold difference in the 20-hydroxyecdysone treated versus untreated parasites, 16% were involved in transcription regulation. Taken together, the transcriptomic, proteomic and phenotypic data suggest that the filarial ecdysone receptor may play a role analogous to that in insects, where it serves as a master regulator of development.

Introduction

Human filarial parasites cause diseases that inflict significant morbidity upon a large proportion of the poorest people on the planet[1]. Lymphatic filariasis (caused by infection with *Brugia malayi*, *Brugia timori* or *Wuchereria bancrofti*) and onchocerciasis (caused by infection with *Onchocerca volvulus*) result in the loss of 5.7 million disability adjusted life years [2]. As a result, these diseases have been identified by the international community as two of the five Neglected Tropical Diseases (NTDs) worldwide, and both have been targeted for elimination by the international community in the London Declaration on Neglected Tropical Diseases [3].

Elimination programs have targeted both onchocerciasis and filariasis have been implemented both at the national and international levels. All rely primarily upon a strategy of mass drug distribution to interrupt transmission and thereby eventually locally eliminate the parasite [4]. However, these programs rely upon the small arsenal of drugs that must be given over a long period of time (*i.e.*, years). This leaves the programs vulnerable to failure in the face of developing resistance. Furthermore, the

prolonged treatment courses necessary to effect elimination presents substantial

logistical difficulties resulting from the need to maintain high drug coverage rates over a

long period of time (i.e. years). Furthermore, the current drug regimens used by these

programs face limitations in deployment in many areas. For example,

diethylcarbamazine (DEC), a drug commonly used to treat lymphatic filariasis produces

severe ocular and systemic complications when given to individuals infected with *O.*

volvulus [5, 6]. This precludes the use of DEC in much of Africa, where lymphatic

filariasis and onchocerciasis are co-endemic. Similarly, treatment of onchocerciasis

using ivermectin is complicated in areas that are co-endemic for the eye-worm *Loa loa*,

as severe adverse events have been documented to occur in individuals treated with

ivermectin that are heavily infected with *L. loa* [7]. For these reasons, there is an urgent

need to develop alternative therapeutic interventions to augment the efforts of the

elimination programs.

Ecdysteroids have long been known to play a central role in controlling the development

of various invertebrates. They have been best characterized in insects. These

hormones exhibit their effects through the activity of ecdysteroid receptors, which act as

master transcriptional regulators [8, 9]. In insects, the juvenile hormones and ecdysone

regulate both embryogenesis and the molting cycle. As the juvenile hormones

decrease, there is a surge in ecdysone levels leading to molting [10]. This effect is

mediated through a heterodimer of the ecdysone receptor (EcR) and the retinoid X

receptor (RXR), two members of the nuclear hormone receptor family of transcriptional

regulators [9, 11, 12]. The fact that molting and the receptors controlling this process

are not found in vertebrates makes this process an attractive potential

chemotherapeutic target.

A homolog of the ecdysone receptor has been identified and shown to be active in

Brugia malayi [13]. However, it's physiological role in controlling the developmental

processes in this parasite remains unclear [13, 14]. To attempt to decipher the

physiological role of the *Brugia malayi* ecdysone receptor (*Bm*EcR), we have conducted

transcriptomic, proteomic and phenotypic studies of the effect on 20-hydroxyecdysone

(20HE) on gravid adult female *B. malayi*.

Materials and Methods

Phenotypic studies of the effect of 20-hydroxyecdysone on fecund adult female worms

Gravid adult female parasites were obtained from the Filariasis Research

Reagent Resource Center (FR3) at the University of Georgia, USA. A total of 5 worms

per well were cultured in a 6-well plate using 3ml of CF-RPMI media (RPMI 1640

supplemented with 25 mM HEPES buffer, 2 mM glutamine, 100 U/ml streptomycin, 100

µg/ml penicillin, 0.25 µg/ml of amphotericin B, and 10% heat-inactivated fetal calf

serum). Experiments were designed to consist of two biological replicates of parasites

treated with 20HE and associated control cultures. When the parasites were received,

they were allowed to acclimatize and monitored for any decrease in motility for 24 hours

(day 0). 20HE was added in the media of the two experimental wells at a concentration

of 10µM on day 1. Control wells received ethanol (the vehicle of 20HE). Media (either

containing or lacking 20HE) was changed every 24 hours, and the parasites cultured for

an additional three days (days 2-4). Three aliquots of 20µl or media were removed from each biological replicate every 24 hours and the life stages released into media were counted, resulting in three technical replicates for each biological replicate for each time point. The life stages observed were counted and classified as microfilariae, pre-microfilariae or eggs/embryos.

Ethics statement

All animal work was conducted according to relevant national and international guidelines outlined by the National Institutes of Health Office of Laboratory Animal Welfare, and was approved under USF IACUC protocol ID: IS00000261

Phenotypic study in gerbils

The phenotypic study was conducted for 150 days with four male Mongolian gerbils maintained in the animal facility at USF under IACUC guidelines. *Brugia malayi* infective larva (L3) was obtained from the Filariasis Research Reagent Resource Center (FR3) at the University of Georgia, USA. Each animal was infected intraperitoneally with 150 L3s under aseptic condition. A total of two experimental animals received 20-hydroxyecdysone (Adipogen, CA) at a dose of 5mg/kg/day/animal for 150 days. The remaining two control animals received ethanol, the vehicle used for delivering 20HE. Alzet mini-osmotic pump Model number 2006 was used provide steady supply of 20HE for 42 days. The pumps were surgically implanted on the dorsal aspect of the gerbils under aseptic conditions two days post-infection. The pumps were replaced every 42 days as per the manufacturer's directions. Hence, each animal received total of 4

31

pumps during the entire study. Peritoneal gavage with 2ml warm and sterile RPMI was performed at 110th day to establish the status of the infection. Animals were euthanized after 150 days post-infection according to IACUC standards using CO_2 gas. Peritoneal gavage was performed to recover microfilariae. Necropsy was conducted to recover adult worms from the peritoneal cavity.

RNA Extraction

Fecund adult females, cultured as described above, were used to prepare RNA for the transcriptome analysis. Total RNA was isolated from the two biological replicates of 5 worms each (2 wells each of treated and untreated parasites) after 2 days culture with and without 20HE. The worms were flash frozen in liquid nitrogen. RNA was extracted from the worms using Trizol LS (Invitrogen, Carlsbad, CA)[15, 16]. The biological replicates of the induced and uninduced samples were lysed individually using TissueLyse II (Qiagen, Valencia, CA) followed by chloroform extraction, isopropanol precipitation and elution in 0.1xTE (1X TE = 10mM Tris-HCl, pH 8.0, 1mM EDTA). The samples were treated with DNase I (Ambion, Austin, TX) according to the manufacturer's instructions. The RNAs were subjected to drop dialysis using 45nm Millipore membranes (EMD Millipore, Billerica, MA) against 0.1 X TE buffer at 4°C for 2 – 4 hours and the RNA then collected from the membranes. The purity of the samples was assessed using a using NanoDrop apparatus (Thermo Scientific, Waltham, MA). The quantity of the RNA was determined using a Qubit apparatus (Life Technologies, Carlsbad, CA). The purified RNA was stored at -80°C.

RNA Library preparation

The NEBNext poly(A) mRNA Magnetic Isolation Module (NEB # E7490) was used to isolate intact poly(A)+ RNA from each previously isolated total RNA. The eluted RNA was used for first and second strand cDNA synthesis using NEBNext Ultra RNA Library Prep Kit for Illumina (NEB # E7530). The double stranded cDNA was size selected and the fractions between 250-550 bp were isolated using 1.8x Agencourt AMPure XP beads. End repair and dA tailing of cDNA library was performed, immediately followed by adaptor ligation. NEBNext Multiplex Oligos for illumina were used for adaptor ligation. The cDNA libraries were PCR amplified and purified. Quality control was performed using a Bioanalyzer (Agilent, Santa Clara, CA) to analyze the quality and size selection of the cDNA. The samples were again subjected to Qubit to quantity the yield of cDNA.

Transcriptome Sequencing

RNAseq was performed on Illumina MiSeq at the Core facility, Smith College, as part of the FR3 (Filarial Reagent Resource Repository), following the manufacturer's protocol. In brief, the cDNA library (at a concentration of 4nM) was denatured using 0.2N sodium hydroxide. The library was diluted to 20pM in Illuminia hybridization buffer, and the template strands hybridized to the adaptors attached to the flowcell surface as previously described [15]. The library was diluted to 9pM with Illumina HT1 buffer. The PhiX control was used as an internal standard. The PhiX standards were denatured and diluted using the same protocol as the sample library. The libraries were heated at 96°C

for 2 minutes, followed by immediate cooling. Samples were loaded into an Illumina cartridge and single-end reads produced.

Data analysis

The Tuxedo suite of programs was used to process and analyze the data [17]. Bowtie2 was used to build indexes of the *B. malayi* reference genome from WormBase (v. WS245)[18]. RNA-Seq reads from each sample were aligned to the *B. malayi* genome using TopHat (v. 1.4.1)[19]. A maximum of one mismatch per read was allowed. The mapped reads from TopHat were used to assemble known transcripts from the reference and their abundances were estimated using Cufflinks [20]. Cuffdiff is very conservative when identifying differentially expressed genes compared to edgeR and DESeq [21]. Thus, edgeR was used to analyze the data using the counts generated for the four samples with Cuffdiff. A heatmap was created using Bioconductor pheatmaps R software comparing the expression of individual transcripts in the 20HE treated and untreated parasites. Gene Ontology (GO) annotations were assigned using WormBase (v. WS245)[22]. Orthologs of the differentially expressed genes from the transcriptome were identified in the *C.elegans* genome using WormBase (v WS249). RNAi phenotypes of the identified *C.elegans* orthologs were assigned using the RNAi tool available at WormBase. Hypergeometric test was performed to obtain the probability of occurrence of the RNAi phenotype in C.elegans genomes as compared to dataset.

Real-Time PCR Validation

Selected genes were chosen based on the GO annotations for real time PCR validation as depicted in Additional file 1 Table 2.1. The gene encoding NADH dehydrogenase subunit 4 (ND4) was utilized as an internal control, as it's expression was equivalent in 20HE induced and control parasites, based upon the transcriptome analysis described above. Three independent biological replicates of control and 20HE treated parasites were prepared as described above. Total RNA was extracted from each replica using the protocol described above. Primers for qRT-PCR were designed to span the exon-intron boundaries, eliminating the possibility of amplification of contaminating genomic DNA in the sample [23]. The primers and probes used for the study are shown in appendix for chapter 1 Table 1. SuperScript® III One-Step RT-PCR System with Platinum® Taq DNA Polymerase (Life Technologies, Carlsbad, CA) was used in the amplification reactions, using the conditions provided by the manufacturer. Taqman chemistry was applied using iTaq Universal Probes One-Step Kit (Biorad, Hercules, CA) for the real time PCR. The efficiency of the PCR reactions using these conditions was calculated to be 95%. Each biological replicate was analyzed using triplicate technical replicates. Relative quantification of starting mRNA copy number in each samples was calculated using the $\Delta\Delta C_t$ method.

Preparation of protein extracts

Adult female worms cultured in the presence and absence of 20HE as described above were homogenized in 150µl of a buffer containing 125mM Tris-HCl (pH 8.5), 4 % SDS 0.5mM PMSF and 100mM DTT. A total of three biological replicates of 20HE

treated and untreated worms were used for the study. Protein concentrations were determined using the Pierce 660 nm Protein Assay supplemented with Ionic Detergent Compatibility Reagent supplementation (Pierce). The samples were processed using Filter-aided sample preparation (FASP) for mass spectroscopy (MS) based proteomic analysis. Raw MS files were processed with MaxQuant with a 1% FDR (False Detection Rate). The normalized ratios of each biological replicate obtained from the MaxQuant analysis were input into the Perseus processing suite [24]. An unpaired student's t-test with a significance value of $p < 0.05$ used to test for statistical significance of the quantitation. A total of 6050 proteins were detected, which included multiple isoforms. Proteins with multiple isoforms were considered as a single entity for further analysis, resulting in 3991 unique proteins. An empirical filter of proteins with more than 2 peptides identified, a p-value less than 0.05 and a greater than 2-fold change was applied to the data. The Bonferroni correction was applied to correct the p-value for the proteins analyzed. A total of 359 proteins were identified to be significantly more abundant in the induced extracts. Gene Ontology (GO) terms were assigned to the differentially abundant proteins.

GO enrichment analysis of the over-represented GO terms

GO enrichment analysis for differentially abundant proteins was performed using the R software environment. All the proteins (19,681) from WormBase were considered as the background list and the differentially abundant proteins identified as described above (359) extracted from the proteomics data were considered as the sample list. A p-value for each GO term, based on its domain was calculated using the

Hypergeometric Test [25]. Enriched GO terms from each domain were sorted based upon a p-value of < 0.05. The top GO terms that were significantly over-represented at least five times more than the control list in the 20HE treated proteins were identified. Graphs were plotted based on ratios of the p-value for the particular GO term and total number of unique proteins exhibiting that category. Biological processes incorporated 200 unique proteins in the ecdysone treated proteome and 1936 in the controls. Molecular processes indicated 155 unique proteins in the 20HE treated proteome and 1620 in the controls.

Results

The role of ecdysone receptor as a master regulator of developmental processes is well discerned in insects. Previous studies with embryos from adult female worm of *Brugia malayi* provided insights of having a functional ecdysone responsive system in culture. To further delineate the role of the ecdysone receptor on the developmental process in a vertebrate host, fecund adult female parasites were initially cultured *in vitro* in the presence and absence of 20HE as described in Materials and Methods. Parasites cultured in the presence of 20HE exhibited a significant increase (p < 0.001) in the production and expulsion of both microfilariae and eggs and embryos when compared to control parasites (Figure 2.1). These data implicated 20HE in the control of microfilarial development and embryogenesis, and provided a phenotype that could be used to monitor the effect of 20HE in subsequent experiments.

An *in-vivo* study was conducted to observe molting and embryological changes, as described in Materials and Methods. After 150 days, the animals were euthanized and the peritoneal cavity was examined for parasites. A total of 25 and 28 adult parasites were recovered from the peritoneal cavity of the control animals. In contrast, the two experimental animals that received 20HE via Alzet mini-osmotic pumps, no parasites were recovered from the first animal whereas a single female was recovered from the second animal. A large number of mature microfilariae were recovered from the controls whereas no microfilariae were observed in the peritoneal cavity of the treated animals. On visual inspection, the adult female parasite recovered from the 20HE treated animal was shorter in length as compared to the control as shown in figure 2.2.

To identify the genes participating in the ecdysone responsive pathways, female *B. malayi* parasites were cultured in the presence and absence of 20HE and harvested after 48 h. This is the time point at which enhanced mf production and expulsion of immature stages from the treated worms were at their peak (Figure 2.1). RNA was then prepared from two independent biological replicates and subjected to transcriptome analysis. The biological replicates demonstrated a strong correlation in their Fragments Per Kilobase of Transcript per Million Mapped Reads (FPKM) values (Figure 2.3, Panel A). Differentially expressed genes were identified using the EdgeR Negative Binomial Distribution as having a minimum of a 2 fold change in expression between the control and treated worms with a p-value <0.01. A total of 44 differentially expressed genes were identified in the 20HE treated parasites when compared to control parasites

cultured in the absence of the hormone; 30 genes were up-regulated and 14 genes were down-regulated (Figure 2.3, Panel B).

Gene Ontology (GO) analysis was performed on the 44 differentially expressed genes. The results of this analysis are summarized in Figure 2.4. A total of 18% of the up-regulated genes were involved in regulation of transcription; 11.3 % participated in cellular processes and 2.27% were involved in cellular differentiation. Of the 30 up-regulated genes, a total of 18 orthologs were identified in the *C.elegans* genome. The RNAi profile of these genes revealed that almost all the orthologs exhibited phenotypes consistent with an involvement in developmental processes, such as embryonic lethal, sterile, reduced brood size, spindle assembly defective early embryos, egg laying defective, L1 arrest, larval arrest, larval lethal, asymmetric cell division defective early embryogenesis, slow growth, pleiotropic defects, severe early embryos, early embryonic lethal and sterile progeny (Table 2.1). The probability of finding embryonic lethal and other embryological phenotypes in the dataset was found to be statistically significant ($p < 0.001$) on hypergeometric test.

To evaluate the quantitative robustness of the transcriptome study, four genes were chosen for validation using q-RT-PCR. These genes were chosen from among the transcriptional regulators identified in the GO analysis, and represented a range of their predicted up-regulation from 5-fold to 392-fold between the treated and untreated. Figure 2.5 shows the fold changes of the three biological replicates of each chosen gene as estimated by q-RT-PCR. The degree of up-regulation seen in the q-RT-PCR

assays were found to correspond closely to those calculated from the FPKM analysis of the transcriptome data in all cases (Table 2.2).   A Pearson correlation coefficient of 0.99 was observed when the degree of up-regulation observed in the transcriptome and qRT-PCR data were compared.

Although the transcriptome analysis demonstrated excellent reproducibility with biological replicates and q-RT-PCR validation, it identified a relatively small number of genes whose transcripts were up-regulated in response to 20HE. However, because protein levels may also be regulated through post-transcriptional mechanisms, the effect of 20HE on the female proteome was also explored. To accomplish this, total protein extracts from adult 20HE treated worms and control worms were subjected to FASP digest and LC/MS/MS spectroscopy, as described in Materials and Methods. A total of 3,991 unique proteins were identified (Additional file 2, Dataset S1). A total of 359 unique proteins were found to exhibit a greater than 2 fold-change in abundance in the 20HE treated parasite extracts when compared to the control worm extracts. These proteins were identified using the annotations provided in WormBase release 240 (Figure 2.6). An overlap of 11 genes was observed between the transcriptomic and the proteomic data. The majority of the proteins that were more abundant in the 20HE extracts had an uncharacterized function. However, similar to what was seen in the transcriptome data, 15% of the more abundant proteins in the 20HE extracts were involved in regulation of transcription. Another 4% were involved in signal transduction, 3% in translation, 3% in chromosomal regulation and cell cycle regulation and 22% in cellular processes. A large number of structural proteins were more abundant in 20HE

treated extracts. The other categories that were more abundant in the treated extracts included protein kinase activity, tyrosine phosphatase activity, and metal ion binding.

GO term enrichment analysis was performed on the proteomic data to determine the significance of the occurrence of the key GO terms whose members were more abundant in the 20HE treated extracts. The key biological processes that were significantly more abundant in the 20HE treated extracts included translation, intracellular protein transport, G-protein coupled receptor protein signaling pathways (Figure 2.7, Panel A). Molecular functions like structural constituents of the ribosome, protein tyrosine phosphatase activity, structural constituents of the cytoskeleton were also identified as more abundant in the treated extracts (Figure 2.7, Panel B).

Discussion

The data presented above suggest that the *Bm*EcR may play a role in embryogenesis in parasitic nematodes, as has been observed in insects. Worms cultured in the presence of 20HE exhibited an increase in expulsion of microfilariae, pre-microfilariae and eggs/embryos into the culture medium for two days, followed by a drop in the number of progeny expelled in subsequent days. These data suggest that 20HE induced abortion of immature life cycle stages from the gravid females, resulting in a depletion of immature parasites from the uterus by the third day in culture. Although the microfilariae expelled into the media in the worms cultured in the presence of 20HE appeared morphologically normal, it was not possible to determine if they were reduced in their ability to infect mosquitoes, as we found that microfilariae produced by gravid

41

females cultured in the absence of 20HE were also not infectious to mosquitoes. Studies measuring the effect of 20HE on infectivity of microfilariae will need to be conducted in a system in which the microfilariae produced are normally infectious (*e.g.,* in infected animals rather than in culture).

The role of the ecdysone receptor on molting and embryogenesis is yet to be described in the human parasite *Brugia malayi*. The *in-vivo* study conducted with L3-stage larva infected gerbils clearly delineates the role of the ecdysone on molting in the host. The implanted parasites failed to develop into adult stage parasites. The effect of 20HE is hypothesized to have caused precocious molting of the L3stage larva. The early molt cycle would have resulted in the death of the organism just like in insects. The parasites recovered control animals were morphologically normal and were actively producing microfilariae. The alone female recovered from the treated animal show clear signs of developmental retardation. The thin body and shorter length provided evidence that eternal stimulation with 20HE causes premature molting leading to developmentally non-viable parasites. The alone female did not show any expulsion of microfilariae. This could be accounted to the fact that there was no male worm to fertilize the eggs. Further studies could be performed to observe the effect of 20HE on gerbils with a patent infection.

A total of 44 differentially expressed genes were identified in the ecdysone-cultured parasites when compared to those cultured in the absence of the hormone. Although few mRNAs were identified as regulated by exposure to 20HE, the data were

robust showing high correlation between biological replicates. Majority of the genes were uncharacterized and unannotated genes. Given the availability of the complete genome with complete annotations and RNAi profiles of all the *C.elegans* genes, orthologs of differentially expressed genes of *B. malayi* were identified in the *C.elegans* genome. As orthologs retain the same functionality during the course of evolution, the results derived from analyzing the RNAi phenotype of the *C.elegans* orthologs could be extrapolated to the *B. malayi* transcriptome. Although few orthologs were identified, almost all of the orthologs revealed a solid phenotypic profiles directing towards numerous embryological events. The data strongly suggests that silencing these particular up-regulated genes can be embryologically detrimental and could lead to death of the parasite. The RNAi phenotype analysis supports the theory that ecdysone receptor regulates embryological events in the human parasite *Brugia malayi*.

To confirm the veracity of the transcriptomic analyses, a series of representative genes whose expression levels were changed by exposure to 20HE were examined using q-RT-PCR. The mean fold change of the three biological replicates of all genes as measured by q-RT-PCR corresponded closely with the mean FPKM values of RNAseq replicates. This suggested that the FPKM values observed in the transcriptome analysis accurately reflected changes in the levels of the various transcripts.

The proteomic data revealed 359 unique proteins whose levels were more abundant in parasites exposed to 20HE. Of these a total of 11 were found to coincide in

the transcriptome and proteome studies. This is similar to other studies in the systems biology literature, which have generally observed few proportional correlations between transcript and protein expression [26-30]. The differences in the transcriptome and proteome datasets could be attributed to different translational efficiencies post-translational regulation and differential protein stability [29, 31-36]. Despite this lack of overlap, the proteomic analysis generally supported the hypothesis derived from the transcriptome data that the *Bm*EcR regulated a regulatory cascade. The proteomic study identified a large number of proteins participating in regulation of transcription, signal transduction and cellular functions as more abundant in worms exposed to 20HE.

Conclusions

In summary, the data presented here demonstrate that 20HE has demonstrable effects of gravid adult female *B. malayi*, at the phenotypic, transcript and protein levels. The RNAi phenotypic analysis strongly suggests that the *Bm*EcR playing a role in regulating embryonic development in this parasite. Further studies will be needed to elucidate the role that this regulator plays in the other life cycle stages of the parasite.

Tables and Figures

Table 2.1: RNAi phenotype analysis of the *B. malayi* orthologs in the *C.elegans* genome.

B.malayi Gene ID	C.elegans Ortholog(s)	RNAi Phenotype(s)
Bm5644	ANMT-1	Embryonic lethal, lethal, sterile
Bm14320	fem-2	Dauer constitutive, embryonic lethal, feminization of XX and XO animals, sterile, reduced brood size, no oocyte, variant, sperm absent
Bm2832	C07H6.4, F10E9.11	Embryonic lethal, spindle assembly defective early embryos
Bm3675	dpm-1, dpm-3	Embryonic lethal, cortical dynamics defective early embryogenesis, sterile progeny, small, sick
Bm5431	egl-15	Bag of worms, egg laying defective, embryonic lethal, L1 arrest, larval arrest, larval lethal
Bm9980	ZK265.7	Embryonic lethal, embryonic lethal, larval arrest
Bm8103	Y18D10A.23, F21D12.3	Reduced brood size, embryonic lethal
Bm58	cnt-2	Asymmetric cell division defective early embryogenesis, embryonic lethal, lethal, reduced brood size, sterile
Bm9280	MNM-2	Axon guidance variant, neuron morphology variant
Bm87	gck-4	Larval arrest, lethal, reduced brood size, slow growth
Bm7925	crh-1	Athermotactic, avoids bacterial lawn, cryophilic, isothermal tracking behavior variant, neuron calcium transient levels variant
Bm14681	dhps-1	Embryonic lethal
Bm11454	Y37E3.10	Pleiotropic defects severe early embryos, sterile, early embryonic lethal, sterile progeny, late embryonic arrest, L1 lethal, sick, lethal, larval arrest, embryonic lethal, nuclear morphology variation early embryos, reduced brood size
Bm432	mif-2	Embryonic lethal
Bm13025	F53E4.1	Maternal sterile
Bm12555	nhr-3, nhr-88	Transgene expression increased
Bm10799	B0336.3	Body wall muscle myosin organization defective, organism development variant, organism morphology variant, slow growth, transgene expression reduced, transgene induced co-suppression variant
Bm8538	fis-1	Egg retention, embryonic lethal

Table 2.2: Comparison of fold change between RNAseq and real time PCR

Gene ID	Putative Functions	RNAseq	qRT-PCR
		I/UI	I/UI
*Bm*58	Signal transduction	8.3	8.4 ± 0.75
*Bm*7925	Regulation of transcription	159.9	169 ± 22.8
*Bm*12555	Nuclear receptor like gene	5.2	4.7 ± 0.38
*Bm*11454	Nematode larval development factor	392	356.5 ± 25.62
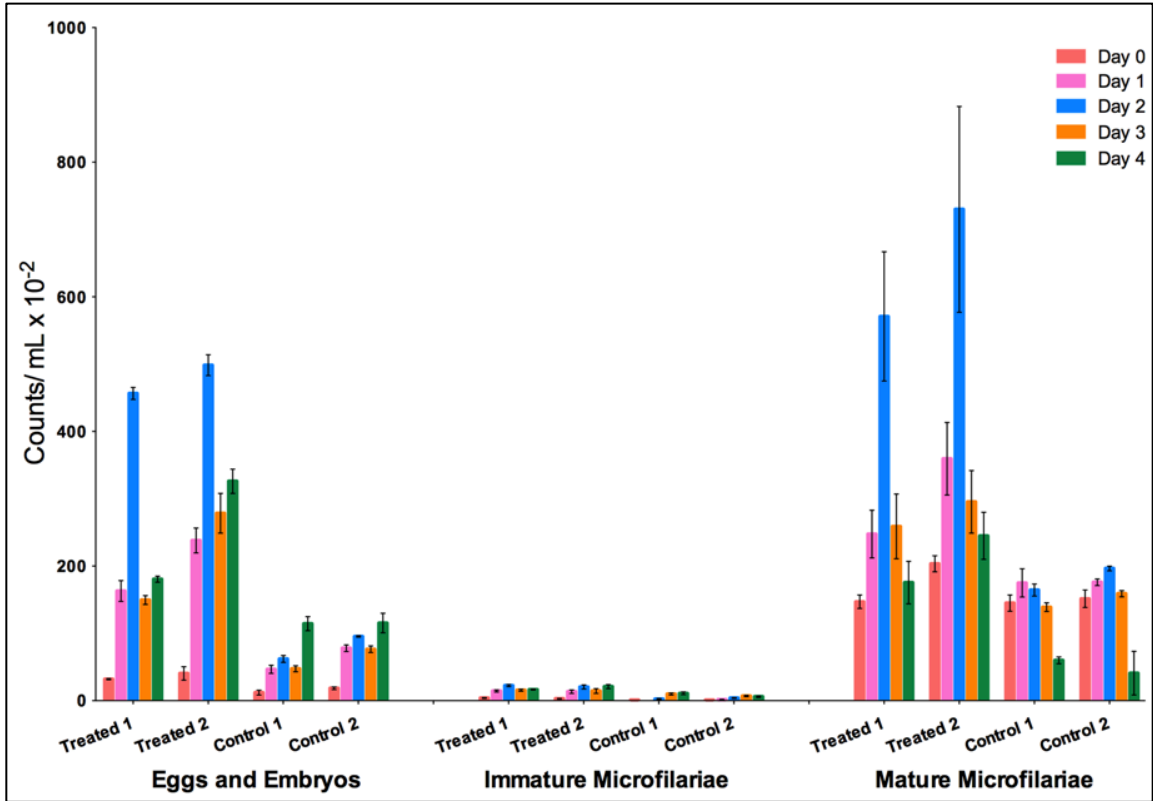
Figure 2.1: Effect of 20-hydroxyecdysone on the physiological activity of the adult female worms in culture: The X-axis shows two biological replicates of the treated and controls. The bars depict counts observed. The error bars show the standard deviation of the three technical replicates.
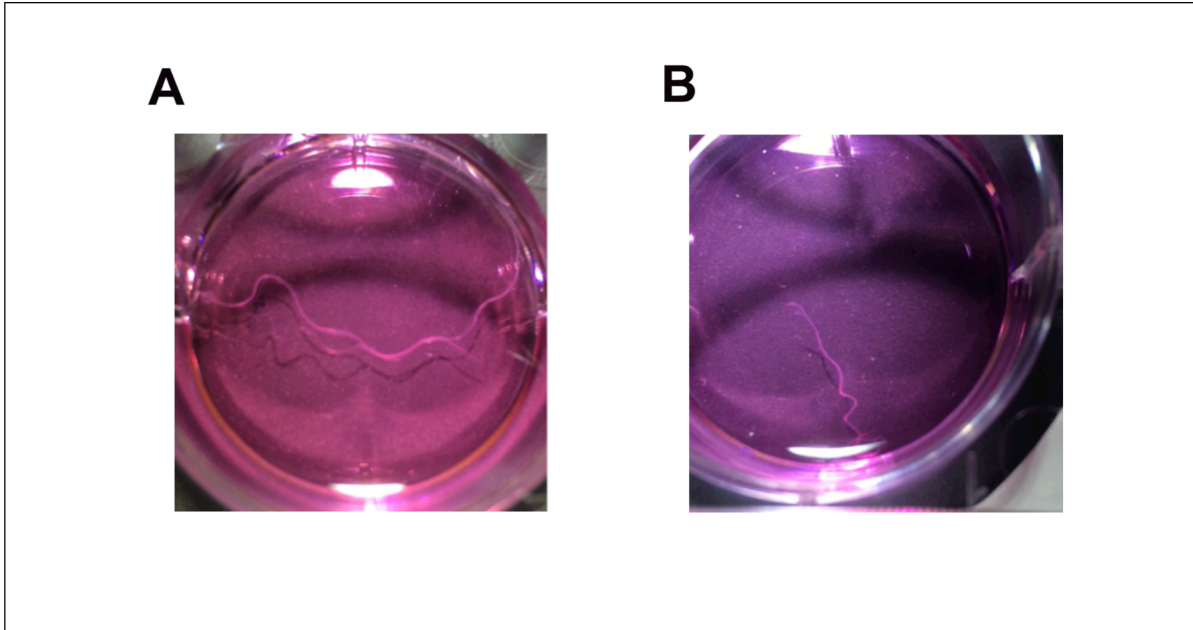
Figure 2.2: *In-vivo* **phenotypic study demonstrating effect of 20HE on adult worms.** Panel A: Control worms showing normal length of the adult female worm. Panel B: Ecdysone treated worms showing stunted growth and shorter length.
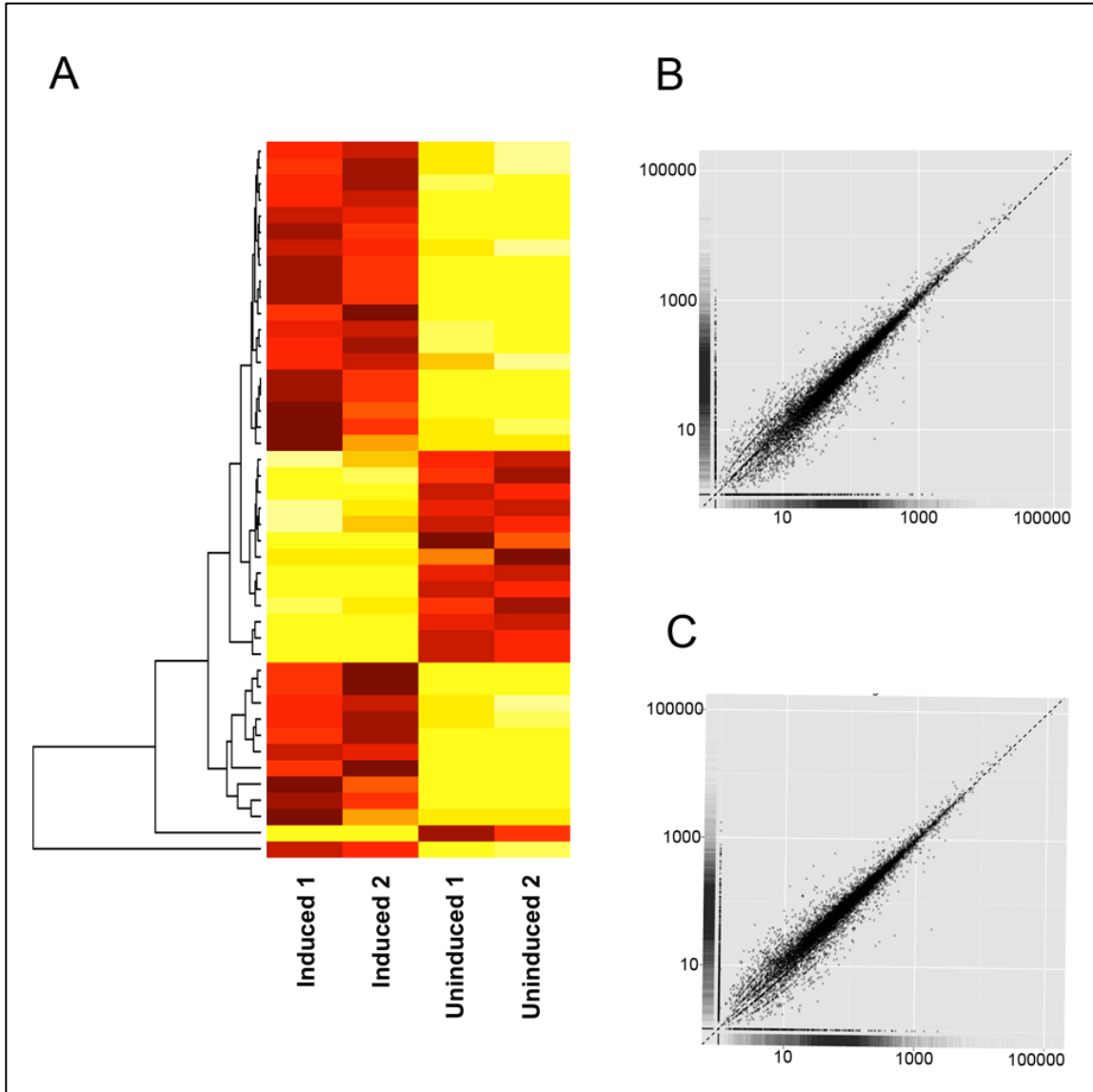
Figure 2.3: Transcriptomic analysis of the 20-hydroxyecdysone induced and uninduced worms. (A) A heat map from hierarchical clustering of differentially expressed genes of the adult female worms induced with 20HE and controls in duplicate experiments (N=4). Expression level was coded as red demonstrating up-regulation and yellow demonstrating down-regulation. **(B)** The scatter plot shows reproducibility of the technical replicate of the induced samples. Expression scores of each biological replicate were plotted on a log10 scale and compared with their counterparts to find any splicing variant in the specific loci. **(C)** The scatter plots shows reproducibility of technical replicates of the uninduced samples.
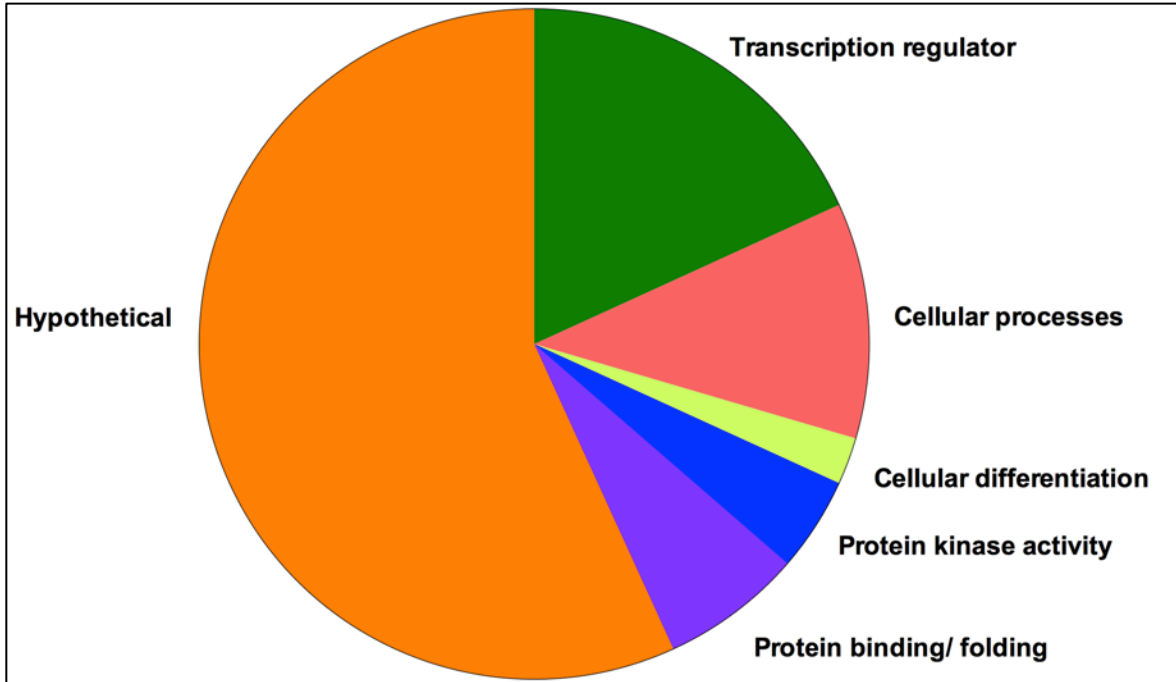
Figure 2.4: Pie chart of the functions of the differentially expressed up-regulated genes: Up-regulated genes were sorted based on the GO classification.
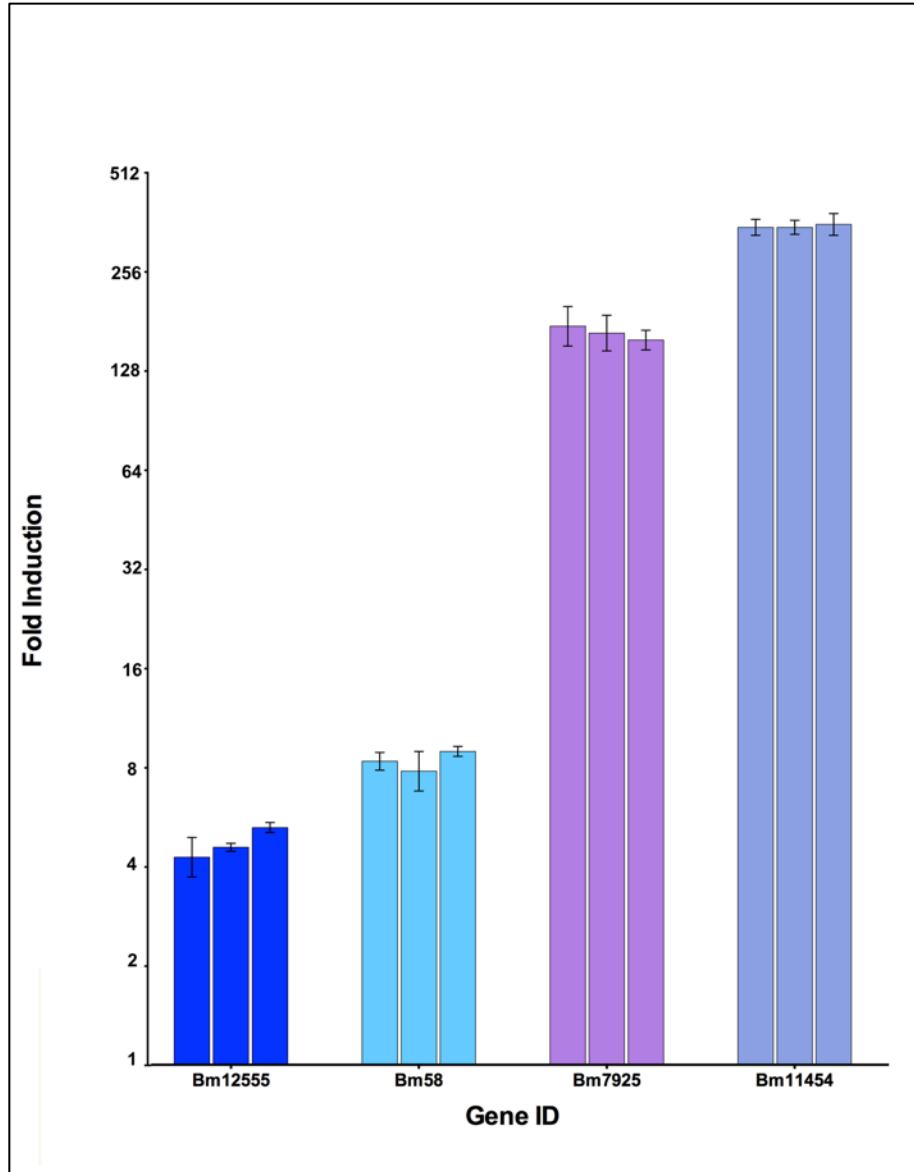
Figure 2.5: qRT-PCR validation of the expression level demonstrated by the RNAseq: Columns represent fold inductions in three biological replicates and the error bars the standard deviation surrounding the estimates of three technical replicates per biological replicate.
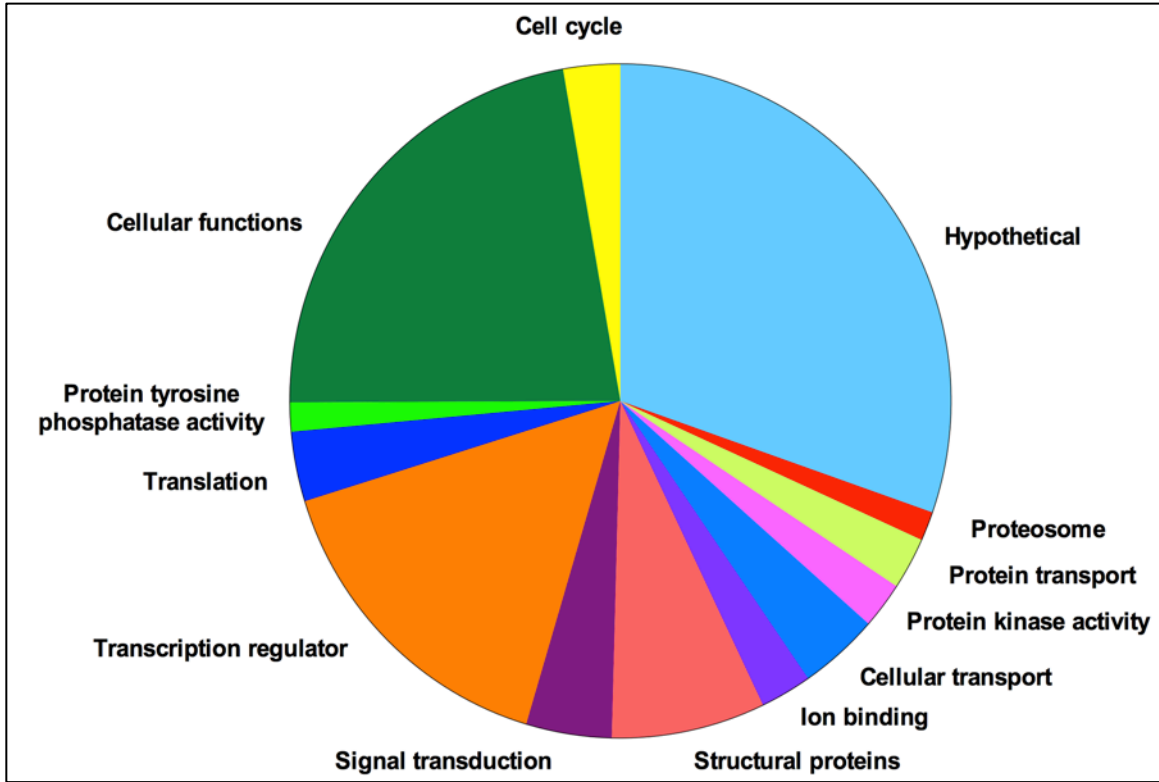
Figure 2.6: Pie chart of the GO terms of the up-regulated proteins: 359 proteins with a greater than 2 peptide match, p-value <0.01 and greater than 2 fold change were included.
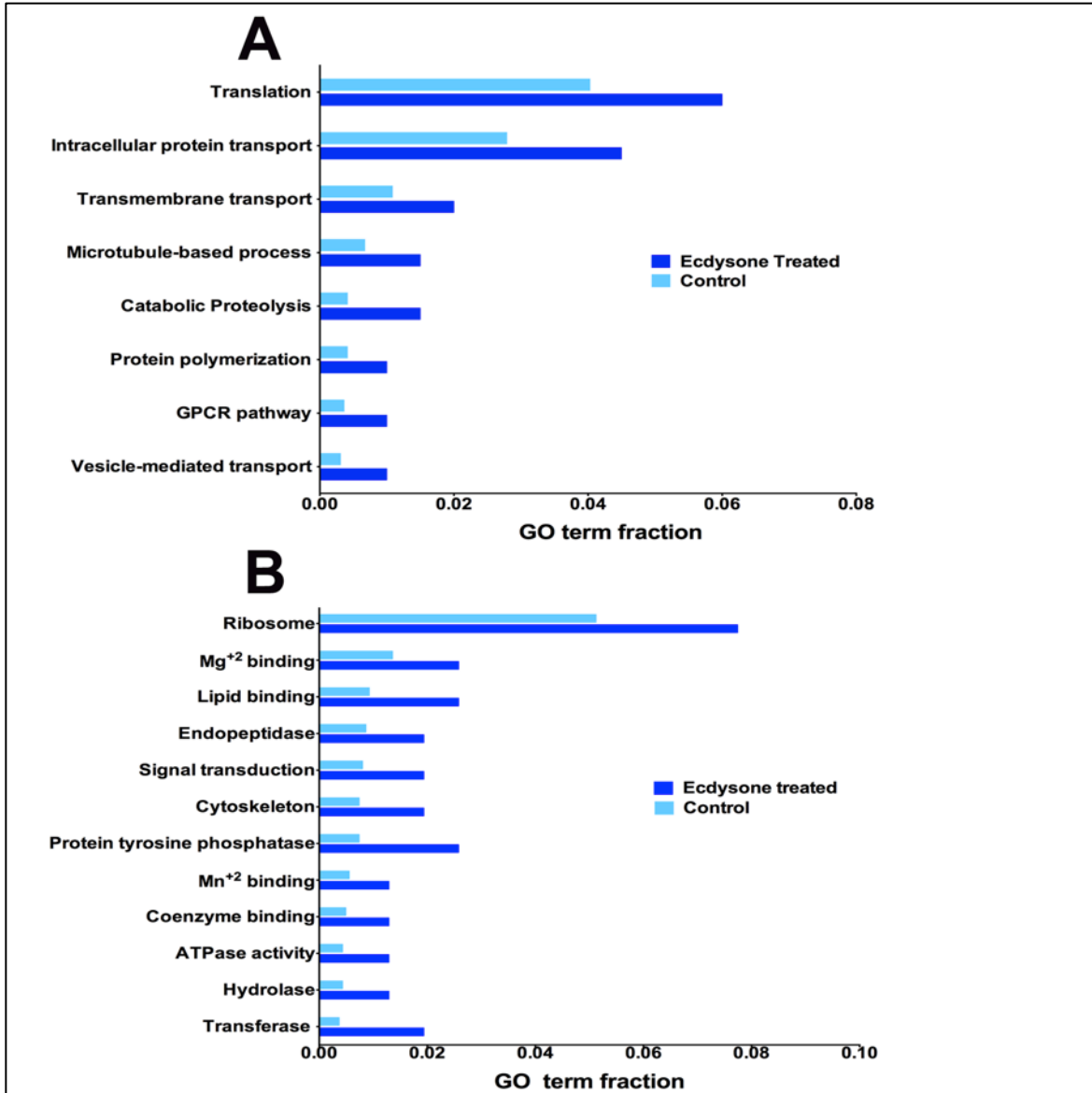
Figure 2.7: Gene Ontology term enrichment analysis of the ecdysone treated proteins as compared with the control. (A) Enrichment for GO 'Biological Process' terms of proteins were detected as more abundant in the induced extracts (dark blue bar) as compared to controls (light blue bar) as determined using Hypergeometric test. The Y-axis shows the terms that were significantly enriched (p-value <0.01). The X-axis displays the fraction relative to all GO Biological Process terms **(B)** Enrichment for GO 'Molecular Function' main terms of proteins were detected as more abundant in the induced extracts (dark blue bar) as compared to controls (light blue bar) as determined using a Hypergeometric test. The Y-axis shows the terms that were significantly enriched (p-value <0.01). The X-axis displays the fraction relative to all GO Molecular Process terms.

References

1. Organization, W.H. *Lymphatic Filariasis - Epidemiology*. 2010 2010 [cited 2010 9-27-2010]; Available from: http://www.who.int/lymphatic_filariasis/epidemiology/en/.

2. Mathers, C.D., M. Ezzati, and A.D. Lopez, *Measuring the burden of neglected tropical diseases: the global burden of disease framework.* PLoS Negl Trop Dis, 2007. **1**(2): p. e114.

3. Turner, H.C., et al., *Reaching the london declaration on neglected tropical diseases goals for onchocerciasis: an economic evaluation of increasing the frequency of ivermectin treatment in Africa.* Clin Infect Dis, 2014. **59**(7): p. 923-32.

4. Cupp, E.W., M. Sauerbrey, and F. Richards, *Elimination of human onchocerciasis: history of progress and current feasibility using ivermectin (Mectizan®) monotherapy.* Acta Tropica, 2011. **120 Suppl 1**: p. S100-8.

5. Awadzi, K., *Clinical picture and outcome of Serious Adverse Events in the treatment of Onchocerciasis.* Filaria J, 2003. **2**(Suppl 1): p. S6.

6. Francis, H., K. Awadzi, and E.A. Ottesen, *The Mazzotti reaction following treatment of onchocerciasis with diethylcarbamazine: clinical severity as a function of infection intensity.* Am J Trop Med Hyg, 1985. **34**(3): p. 529-36.

7. Twum-Danso, N.A., *Serious adverse events following treatment with ivermectin for onchocerciasis control: a review of reported cases.* Filaria Journal, 2003. **2**(Suppl 1): p. S3.

8. Baehrecke, E.H., *Ecdysone signaling cascade and regulation of Drosophila metamorphosis.* Archives of Insect Biochemistry and Physiology, 1996. **33**(3-4): p. 231-44.

9. Koelle, M.R., et al., *The Drosophila EcR Gene encodes an ecdysone receptor, a new member of the steroid receptor superfamily.* Cell, 1991. **67**: p. 59-77.

10. Riddiford, L.M., *Hormone receptors and the regulation of insect metamorphosis.* Receptor, 1993. **3**(3): p. 203-9.

11. Yao, T.P., et al., *Functional Ecdysone Receptor Is the Product of EcR and Ultraspiracle Genes.* Nature, 1993. **366**(6454): p. 476-479.

12. Thomas, H.E., H.G. Stunnenberg, and A.F. Stewart, *Heterodimerization of the Drosophila ecdysone receptor with retinoid X receptor and ultraspiracle.* Nature, 1993. **362**(6419): p. 471-5.

13. Tzertzinis, G., et al., *Molecular evidence for a functional ecdysone signaling system in Brugia malayi.* PLOS Neglected Tropical Diseases, 2010. **4**(3): p. e625.

14. Mendis, A.H., et al., *Ecdysteroids in adults of the nematode, Dirofilaria immitis.* Mol Biochem Parasitol, 1983. **9**(3): p. 209-26.

15. Choi, Y.J., et al., *A Deep Sequencing Approach to Comparatively Analyze the Transcriptome of Lifecycle Stages of the Filarial Worm, Brugia malayi.* PLoS Negl Trop Dis, 2011. **5**(12): p. e1409.

16. Griffiths, K., et al., *Use of microarray hybridization to identify Brugia genes involved in mosquito infectivity.* Parasitology Research, 2009. **106**(1): p. 227-235.

17. Trapnell, C., et al., *Differential gene and transcript expression analysis of RNA-seq experiments with TopHat and Cufflinks.* Nat. Protocols, 2012. **7**(3): p. 562-578.

18. Langmead, B., et al., *Ultrafast and memory-efficient alignment of short DNA sequences to the human genome.* Genome Biol, 2009. **10**(3): p. R25.

19. Trapnell, C. and S.L. Salzberg, *How to map billions of short reads onto genomes.* Nature biotechnology, 2009. **27**(5): p. 455-457.

20. Trapnell, C., et al., *Transcript assembly and quantification by RNA-Seq reveals unannotated transcripts and isoform switching during cell differentiation.* Nat Biotechnol, 2010. **28**(5): p. 511-5.

21. Seyednasrollah, F., A. Laiho, and L.L. Elo, *Comparison of software packages for detecting differential expression in RNA-seq studies.* Briefings in Bioinformatics, 2013.

22. Gentleman, R.C., et al., *Bioconductor: open software development for computational biology and bioinformatics.* Genome Biol, 2004. **5**(10): p. R80.

23. Ye, J., et al., *Primer-BLAST: a tool to design target-specific primers for polymerase chain reaction.* BMC Bioinformatics, 2012. **13**: p. 134.

24. Bell-Temin, H., et al., *Quantitative proteomic characterization of ethanol-responsive pathways in rat microglial cells.* Journal of proteome research, 2013. **12**(5): p. 2067-77.

25. Rivals, I., et al., *Enrichment or depletion of a GO category within a class of genes: which test?* Bioinformatics, 2007. **23**(4): p. 401-407.

26.   Ghazalpour, A., et al., *Comparative analysis of proteome and transcriptome variation in mouse.* PLoS Genetics, 2011. **7**(6): p. e1001393.

27.   Chen, G., et al., *Discordant protein and mRNA expression in lung adenocarcinomas.* Mol Cell Proteomics, 2002. **1**(4): p. 304-13.

28.   Pascal, L.E., et al., *Correlation of mRNA and protein levels: cell type-specific gene expression of cluster designation antigens in the prostate.* BMC Genomics, 2008. **9**: p. 246.

29.   Yeung, E.S., *Genome-wide correlation between mRNA and protein in a single cell.* Angewandte Chemie (International ed. in English), 2011. **50**(3): p. 583-5.

30.   Darby, A.C., et al., *Analysis of gene expression from the Wolbachia genome of a filarial nematode supports both metabolic and defensive roles within the symbiosis.* Genome Research, 2012. **22**(12): p. 2467-77.

31.   Haider, S. and R. Pal, *Integrated Analysis of Transcriptomic and Proteomic Data.* Current Genomics, 2013. **14**(2): p. 91-110.

32.   Grossman, A.D., et al., *Mutations in the rpoH (htpR) gene of Escherichia coli K-12 phenotypically suppress a temperature-sensitive mutant defective in the sigma 70 subunit of RNA polymerase.* Journal of bacteriology, 1985. **161**(3): p. 939-43.

33.   Gustafsson, C., S. Govindarajan, and J. Minshull, *Codon bias and heterologous protein expression.* Trends in biotechnology, 2004. **22**(7): p. 346-53.

34.   Greenbaum, D., et al., *Comparing protein abundance and mRNA expression levels on a genomic scale.* Genome biology, 2003. **4**(9): p. 117.

35.   Cho, R.J., et al., *A genome-wide transcriptional analysis of the mitotic cell cycle.* Molecular cell, 1998. **2**(1): p. 65-73.

36.   Hargrove, J.L. and F.H. Schmidt, *The role of mRNA and protein stability in gene expression.* FASEB journal : official publication of the Federation of American Societies for Experimental Biology, 1989. **3**(12): p. 2360-70.

CHAPTER THREE

ECDYSONE RECEPTOR: A NOVEL TARGET FOR DEVELOPMENT OF DRUGS AGAINST LYMPHATIC FILARIASIS

Abstract

A homologue of the ecdysone receptor (EcR), a master regulator of development in insects has previously been identified and shown to be responsive to 20HE (20-hydroxyecdysone) in transfected *B. malayi* embryos. As the EcR is not found in vertebrate animals, it and the regulatory pathways it controls represent an attractive potential chemotherapeutic target. A mammalian two-hybrid system involving *Bm*EcR Gal4 and RXR VP16 fusion constructs and a GAL4 *Gaussia* luciferase reporter was used in the transient transfection assay. When bound to a cognate ligand like 20-hydroxyecdysone, transactivation of the luciferase reporter is observed. A stable cell line was created incorporating the three plasmids in the HEK293 cell line genome for the development of a high throughput screening assay to identify agonists and antagonists of the filarial EcR. The assay was employed to screen steroidal, non-steroidal and natural ecdysone analogs. A total of 7 agonists and 2 antagonists have been identified. A homology model was created using the *Bm*EcR ligand-binding domain for virtual docking studies. The homology model was used to study the ligand-

receptor interaction of the agonists identified with the molecular assay. An excellent correlation between the homology model and the molecular assay was observed. Based on both the screening models, the diacylhydrazine family of compounds was identified as a fruitful source of potential agonists or antagonists of the receptor. These studies should assist in the development of inhibitors for the *Bm*EcR that may be evaluated as potential lead compounds for development of a new class of drugs against the filariasis.

Introduction

Diseases caused by the human filarial parasitic nematodes are a significant public health problem faced by developing countries. Recent reports estimate that there are over 140 million individuals suffering from human filarial parasites in over 80 countries worldwide. Even larger numbers of individuals (> 1 billion) remain at risk for contracting the filarial infections [1]. Lymphatic filariasis (caused by infection with *Brugia malayi, Brugia timori* or *Wuchereria bancrofti*) and onchocerciasis (caused by infection with *Onchocerca volvulus*) result in severe debilitating diseases together resulting in a loss of 5.7 million disability adjusted life years [2].

Both lymphatic filariasis (LF) and onchocerciasis have been designated as neglected tropical diseases by the international community and both have been targeted for elimination in the London Declaration on Neglected Tropical Diseases [3]. The efforts to eliminate LF and other NTDs have generally relied on mass drug administration (MDA) programs. Though MDA programs have on the whole been well formulated and executed, they face potential challenges that may threaten their ultimate

success. These include the development of resistance to the limited number of drugs that are deployed by the MDA program [4] and local clinical limits on the use of MDA in certain areas. For example, diethylcarbamazine (DEC) is used to treat LF by MDA programs throughout India, South America and Southeast Asia [5, 6]. However it cannot be used in Africa, as it causes severe ocular side effects and systemic complications in individuals co-infected with *O. volvulus*, the causative agent of onchocerciasis, a disease that is endemic throughout most of sub-Saharan Africa [7, 8]. Similarly, ivermectin, which is the only drug used by the MDA programs worldwide to treat onchocerciasis, cannot be easily used in much of Central Africa.   This area is endemic for the eyeworm *Loa loa*, and treatment of *L. loa* infected individuals with ivermectin can result in to severe neurological reactions, including coma and death [9]. Thus, new and diversified treatments are desperately needed to treat these infections.

Ecdysteroids are master regulators of development in insects, and are thought to also play a central role in controlling development in other organisms in which molting is a central feature of the life cycle (the ecdysozoans)[10]. In insects, molting and other developmental processes (including embryogenesis) are controlled through variation in the levels of the molting hormones, or ecdysteroids, which induce molting and the juvenile hormones, which inhibit molting [11, 12]. This process is mediated through a heterodimer of the ecdysone receptor (EcR) and the retinoid X receptor (RXR), which controls the transcriptional activity of the developmental genes regulating ecdysis [13]. The fact that ecdysis is the central developmental pathway in insects and is a pathway totally lacking in vertebrates has made it an attractive target for the development of

compounds that might act selectively against invertebrates [14, 15]. Thus, the agricultural industry has targeted the EcR in pesticide development in the past, as insects represent one of the largest classes of ecdysozoans on Earth. The narrow window of activity against a specific pest species makes it an excellent target for pest management agents. For example, tebufenozide has insecticidal activity against lepidopteran pests but shows no activity against the hymenopteran insects [15].

A homolog of the EcR has been identified and proven to be functional in *Brugia malayi* [10, 16]. Homologues of the EcR have also been identified in the genomes of other human filarial parasites. The physiological role played by ecdysone receptor remains unknown. However previous studies have demonstrated that treatment of the filaria with ecdysteroids can affect embryogenesis [16], molting[17] and viability of adult parasites, suggesting that the EcR might represent an attractive chemotherapeutic target against these infections. In this study, we report progress towards the development of a high throughput screening assay to identify agonists and antagonists against the *Bm*EcR, the results of a preliminary screen of known steroidal analogs active against other members of the NHR family, and the development of a homology model of the *Bm*EcR that will be useful in conducting *in-silico* screens for agonists and antagonists of the *Bm*Ecr and in optimizing leads identified by high throughput and *in-silico* approaches.

Materials and Methods

Transient transfection of HEK293 cells

Previous studies utilized a system in which plasmids were transiently transfected into NIH3T3 cells [10]. However, in these studies the plasmids were transfected into HEK293 cells due improved growth and enhanced assay characteristics when these cells were used. The cells were grown in 1x MEM (Cellgro, MA) growth media fortified with 10% heat inactivated fetal bovine serum (Atlanta Biologicals, GA), and 1% Penicillin-Streptomycin (100x stock from Thermo-Fisher, MA). The cells were maintained in tissue culture treated T75 flasks (Corning Inc, NY) at 37°C and 5% CO_2. Transient transfection studies utilized previously described constructs [3] consisting of three plasmids: 1. A plasmid encoding the ligand binding domain (LBD) of the *Bm*EcR fused to the GAL4 DNA binding domain at a concentration of 150ng/well; 2. A plasmid encoding a dimerization partner consisting of the human RXR chimera fused to the VP16 activation domain at a concentration of 100ng/well; and 3. A reporter construct containing a minimal promoter, a GAL4 activation domain, and five copies of the ecdysone response element driving the transcription of a secreted *Gaussia princeps* luciferase open reading frame at a concentration of 150ng/well [10]. The plasmids were chemically transfected in the cells using the Lipofectamine® LTX and Plus™ reagent (Invitrogen, CA). DNA-lipid complexes were formed by incubating the three plasmids (at the above concentrations) with 1.5ul of LTX reagent per well and 0.5ul of Plus reagent per well at room temperature for 20 minutes. In brief, 50,000 cells were seeded in each well of a standard 96 well tissue culture plate (Costar, Sigma-Aldrich, MO). The plate was incubated for 18-24 hours. When the cells reached an optimum density of 70-90%,

the DNA-lipid complex was added to each well. The cells were further incubated for 24 hours and 20HE dissolved in ethanol (vehicle) was added at a final concentration of 10uM to half the wells. The other half of the wells received ethanol alone. The plate was incubated at 37°C under 5% CO_2 for an additional for 48 hours. A total of 10ul of the supernatant culture media was removed from each well and assayed for the presence of *Gaussia* secreted luciferase using the Dual Luciferase assay kit (Promega, WI) and measuring absorbance for renilla luciferase at 480nm wavelength as following the manufacturer's protocol. Z' values for the assay were calculated using the formula [18].

$$Z' = 1 - \frac{3(\sigma p + \sigma n)}{|\mu p - \mu n|}$$

Constructs for creating stable cell line

To adapt the transient transfection assay into a high throughput screen, a stable mammalian cell line was developed, in which all three of the necessary constructs were integrated into the mammalian genome, employing the Gateway recombination system (Invitrogen, CA). In brief, three cassettes were constructed. The first cassette consisted of the LBD of the *Bm*EcR fused to a heterologous GAL4 DNA binding domain. This fusion ORF was placed under the control of the CMV intermediate early promoter and terminated with an Sv40 poly-A addition signal. The second cassette contained the ORF for the human RXR chimera fused to the VP16 activation domain. This chimeric ORF was placed under the control of the SV40 promoter and terminated with the bovine growth hormone poly-A addition signal. Finally, the *Gaussia princeps* secreted luciferase reporter ORF was flanked by a GAL4 response element, five copies of the ecdysone response element and a minimal promoter. The reporter ORF was terminated with the human B globin poly-A addition signal. All cassettes were prepared using

standard molecular cloning procedures and amplified by PCR with appropriate primers to produce products ready for recombination cloning. The three cassettes were then cloned by recombination into three pDONR vectors of the multisite Gateway Pro system (Figure 3.1). The sequence of the resulting entry clones were confirmed and the functionality of the entry clones confirmed by transiently transfecting all three into HEK293 cells and testing for reporter activity in cells cultured in the presence and absence of 20HE, as described above. The entry vectors were then inserted by three-way recombination into the destination vector pJTI Fast Dest (Invitrogen, CA) to create a destination vector containing all three cassettes (Figure 3.1). This construct was validated by DNA sequencing and by functional assays, as described above. The destination vector was then used to create a stable mammalian cell line in HEK293 cells, using the Jump In Fast Gateway Targeted Integration System (Invitrogen, CA). Clones were selected in the presence of 30ug/mL hygromycin, following the manufacturer's protocol, and individual clones selected and screened for reporter expression in the presence and absence of 20HE, in order to identify the clone producing the greatest signal to noise ratio and minimal well-to-well variation. The clone that exhibited highest signal to noise ratio was cultured and maintained in T75 flasks using 1x MEM media fortified with 10% FBS.

Screening strategy and screening of ecdysone analogs

Thirty-five thousand seeded cells of the cell line developed as described above were seeded into each well of a 96 well tissue culture plate. The cells were grown under the same conditions as mentioned above. Cells were incubated at 37°C for 18-24 hours

until they reach optimum density of 70-90%. Compounds were added to wells containing the cells at a concentration of 10uM and the cells incubated in the presence of the compounds for 48 hours. Control wells received ethanol, the vehicle of 20HE. A total of 10ul of the culture media was removed from each well and assayed for secreted luciferase activity as described above.

The strategy for assaying for agonist and antagonist activity against the *Bm*EcR is summarized in Figure 3.2. In brief, each compound was assayed in triplicate in cells that were incubated in the presence or absence of 10uM 20HE. Compounds were considered to have agonist activity if they resulted in a significant increase in reporter activity when added to cultures of the stable reporter cells cultured in the absence of 20-HE. They were considered to have antagonist activity if they resulted in a significant decrease in reporter activity when added to cultures of cells that were already cultured in the presence of 20HE. The student t-test was used to calculate the significance of any agonist or antagonist activity observed, and the Bonferroni correction was applied to the results to correct for multiple comparisons. The compounds that resulted in a statistically significant increase or decrease in reporter activity ($p < 0.05$, Bonferroni corrected) were further cultured with the cells in the ten-fold serial dilutions in triplicate format to calculate EC_{50} values. To assess cytotoxic effects of the compounds on the mammalian cell line, cell viability was assayed with Alamar Blue (Thermo-Fisher Scientific, MA) according to manufacturers protocol

Homology model construction, validation and refinement

Figure 3.3 presents the pipeline used to generate the homology model. The
tertiary structure of the *Bm*EcR was predicted using the Schrödinger's Prime 3.1
comparative homology modeling module (Prime. Schrodingers, LLC New York, NY
version 3. ed. 2012). Due to the lack of experimental crystal structure, a search for
suitable template structures upon which to model the *Bm*EcR was undertaken using
BLAST (basic local alignment search tool)[19]. The hemipterin *Bemisia tabaci,* EcR
(PDB ID: 1Z5X) was predicted to be the best template homolog of *Bm*EcR (BLAST-bit
score: 145.2). Based on the template secondary structure, Clustalω [20] was used to
optimize the placement of *Bm*EcR LBD α-helices and β-sheets using a hidden Markov
model (HMM). After the Clustalω alignment studies, backbone atoms for aligned regions
and conserved residue side chain atoms were directly transferred from the template to
the query sequence to create an initial structure, followed by adding insertions and
closing gaps using a knowledge based approach. The *B. tabaci* EcR native substrate
ponesterone A was retained in the binding site during the homology model construction.
The prime serial loop sampling protocol was used to refine one particular loop of
importance (residues 162-175) that constitutes part of the binding site. To alleviate
possible steric clashes between residues after model construction, Truncated Newton
Conjugate Gradient (TNCG) minimization was performed in implicit solvent (VSGB 2.0)
with OPLS-2005 force-fields, until convergence was reached (< 0.01 kcal.mol^{-1} Å^{-1})[21].
The homology model was validated by generating Ramachandran plots and compared
to the homology model generated using I-Tasser web-server (details in supplemental
material) for structural validation [22]. To further improve the quality of homology model,

Molecular Dynamic (MD) simulations were performed for 65 ns evaluating structural properties such as radius of gyration (R_g), root mean square deviation (RMSD), root mean square fluctuation (RMSF) and total energy of the system (details in supplemental material). A representative structure was generated by choosing the compound with the lowest interaction energy from the highly populated clusters for performing docking studies (see supplemental material for details).

Molecular Docking studies

All ligand structures were optimized implementing Schrödinger's LigPrep 2.3 module to produce appropriate 3D structures with correct stereochemistry, protonation states, and ring conformations. The optimized ligands were then virtually docked in the *Bm*EcR homology model using Glide 5.8 docking program. Glide uses a user-defined grid to determine the shape and properties of the binding site. The *Bm*EcR grid was defined by selecting the center of ponasterone A with otherwise default settings. The ligands were first docked and scored according to Glide SP (standard precision) and then re-docked with Glide XP (extra-precision) protocol. Glide Scores (GScores) were calculated to estimate the relative binding affinity amongst the ligands for the EcR binding site [23]. As part of the default Glide docking procedure, the van der Waals radii of non-polar hydrogens were scaled by a factor of 0.8 and all calculations were performed with the OPLS-2005 force fields.

Results

As a first step in identifying lead compounds that were capable of inappropriately

inactivating or inhibiting the *Bm*EcR, an assay based upon transient transfection of

mammalian cells with the *Bm*EcR, a heterodimeric partner and a secreted *Gaussia*

luciferase reporter was developed. This assay was based upon batch transfection of

HEK293 cells will three plasmids, followed by culture of the transfected cells in the

presence of 20HE, a known ligand capable of activating the *Bm*EcR [3]. The mean

luciferase activity in the media of cells exposed to 20HE ranged from 6.93 to 8.2 fold

when compared to the media of cells cultured in the absence of 20HE The Z' value of

the assay ranged between 6.7- 7.3 (Figure 3.4, Panel A). These preliminary studies

demonstrated that the transfected mammalian cell assay has the potential of being used

to screen for agonists and antagonists of the *Bm*EcR. However, transient transfection

of mammalian cells exhibited variation from day to day, and required repeated

transfections of cells, both of which were impediments to adapting the assay to a high

throughput format. To overcome these obstacles, a stable cell line was created that

incorporated the three cassettes necessary for the assay (the *Bm*EcR LBD, the RXR

partner and the reporter) into the genome of HEK293 cells. Assays using these cells

cultured for 24 hours in the presence or absence of 20HE revealed a performance

comparable or better than that of the assay using the transiently transfected cells, with a

signal to noise ratio ranged from 4.5 to 5.5 and a Z' that ranged from 0.78 to 0.88 of the

assays when conducted on different days (Figure 3.4, Panel B).

The stable cells were used to screen a focused library comprising of 40 compounds belonging to the diacylhydrazine (DAH), tetrahydroxyquinolone and the steroidal ecdysone analog families. These compounds were tested for agonist or antagonist activity against *Bm*EcR using the screening strategy mentioned in Materials and Methods. The initial screen identified seven compounds as agonists that resulted in a significant increase in reporter activity in the stable cells cultured as compared to cells cultured in the presence of solvent alone (Figure 3.5, Panel A; $p < 0.05$, with Bonferroni correction for multiple comparisons). Muristerone and Ponasterone A demonstrated a level of agonist activity than the positive control 20HE on the mammalian stable cells. Two compounds were identified as antagonists i.e. those that that resulted in a significant decrease in reporter activity when added to cells cultured in the presence of 20HE when compared to cells cultured in the presence of 20HE alone (Figure 3.5, Panel B $p < 0.05$, with Bonferroni correction for multiple comparisons).

The compounds identified as agonists were then tested at a series of concentrations to determine EC_{50} values for each. EC_{50} values for the initial hits all were low, with some exhibiting values that were in the sub-uM range (Figure 3.6). The agonists were also tested for cytotoxicity as described in Materials and Methods. None of the compounds exhibited cytotoxicity at a concentration of 10 uM.

A homology model of the *Bm*EcR LBD was then created as described in Materials and Methods. The Ramachandaran plots before and after MD simulations were created to observe changes in phi-psi distributions. The number of residues within

the favored and allowed regions increased from from 89.6%to 98.7% as a result of this process (details in supplemental material). Figure 3.7 presents structure of the *B. malayi* EcR LBD homology model with ponasterone A occupying the active site.

The homology model was used for virtual screening studies of agonists identified with the molecular assay above to verify the model performance. The structure with the most favorable protein – ligand interaction energy based on the MD simulation (according to an RMSD clustering scheme of the final 20 ns) was chosen as the representative structure for molecular docking studies. The 3D structures of the ligands were docked and scored using both Glide SP (standard precision) and Glide XP (extra precision) (Figure 3.8). The predicted lowest energy for each agonist (ligand) is described in detail in the supplemental material (see SI). A comparison of computational and experimental results is shown in Table 3.1. A Pearson correlation coefficient of 0.78 was found between experimental log EC_{50} values and Glide XP docking scores, suggesting that the model predictions conformed well with the data collected from the mammalian cell assay.

Discussion

The experiments described in the first chapter of this thesis have demonstrated that 20HE has effects on both embryogenesis and development of *B. malayi* from the infective larvae stage to the adult stage, suggesting that homologues of 20HE may represent an important potential chemotherpeutic space for the development of new drugs against the human filaria. Here, we have described the development of a simple

assay with characteristics that make it compatible with a high throughput screening format and a homology model for in silico screening that together may be used to identify agonists or antagonists targeting the *Bm*EcR.

As described above, the initial optimization if the assay involved cells transiently transfected with three individual plasmids. While this assay demonstrated a good signal to noise ratio and an acceptable Z' value, this assay required producing transfeced cells on a daily basis a peocess that was both cumbersome and subject to day ot day variations. For this reason, we developed a cell line into shich all three of the necessary cassettes were inserted into the host cell's genome. This assay exhibited performance characteristics that equalled or exceeded those of the original assay, but made the assay much more amenable to a high throughput format.

As a first test of the assay, a small library of compuonds that has perviously been shown to act as ligands for EcRs of other species, as well as ligands for other members of the NHR family were screened for activity aginst the *Bm*EcR. The results of this study suggested that members of the diacylhydrazne family were identifed as ecdysone analogs for the *Brugia malayi* EcR. This class of compounds has been exploited the agricultural industry to develop insecticides targeting insect EcRs that cause precocious molting, leading to the death of the the target organism. The DAH bind exclusively to the ligand binding domain of the ecdysone receptor. These compounds show high species specificity. For example, tebufenozide binds with the lepidopteran ecdysone receptor resulting in precocious molting and death of the insect whereas it does no show any

activity against the hymenopteran insects ecdysone receptor. There is no evidence of detrimental effects of DAH on the vertebrates. The lack of the ecdysone receptor in the vertebrates and the species specificity of the DAH make them good chemotherapeutic agents for application in the field for treating and preventing lymphatic filariasis. Further studies need to be performed to observe the activity of the compounds identified in an animal model to guage the performance and efficacy. Other families of compounds like tetrahydroquinolones(THQ), butyl-benzamide and acylaminoketone (AAK) have been known to be ecdysone agonist. Compounds from these families need to be tested for activity against the ecdysone receptor. Focused libraries include compounds showing activity against nuclear hormone receptor family, natural extracts from plants and fungii, FDA approved drugs and the MMV box could potentially used for screening purposes. High throughput screening could also be used to identify novel scaffolds binding the receptor. Further, the compounds could be tested individually for activity. Testing of these ecdysone analog families and different libraries are essential to identify hits and further develop the drug for use.

To complement the high throughput assay described above, a homology model was created for in silico screening of potential ligands against the *Bm*EcR. When using homology models to predict ligand binding, it is important to verify if the resulting models are a) likely to be found in nature, b) structurally relatable to other proteins in their family (i.e., have the same overall fold), and c) are reproduceable. Thus, with Ramachandaran plots and direct comparison to known protein relatives and a model produced by a third party, a fairly confident estimate is made that the binding site of the constructed model

of the *Bm*Ecr LBD likely represents the true binding site. Additionally, the *B. malayi*

EcR-LBD's mechanism is taken into consideration in the model, in that upon binding of

20-hydroxyecdysone to the EcR LBD, a conformational change allows H12 to interact

with molting promoter sequence on DNA, which then facilitates DNA transcription of

molting genes. A protein's structure and function are intimately related, and thus the fact

that the procedure was able to capture one of the key functional elements of the EcR

provides added support for the potential utility of our model in virtual screening studies.

The *B. malayi* EcR model was simulated in the NPT ensemble for 65 ns to

ensure the model was stable and to allow the model to access more relaxed

conformations. RMSF analysis of all residues illustrated that amino acids within the

binding site were particularly inflexible with most values < 2Å, which indicates that these

residues have optimized favorable interactions amongst themselves. Out of the

converged portions of simulation (i.e., the last 20 ns of simulation) a RMSD clustering

scheme (as described in the Methods) was employed to find a snapshot that was

representative of the entire simualtion. This snapshot (less ponasterone A) was used as

the binding site in virtual screening studies.

In the analysis of predicted binding poses for each ligand, a pattern was

observed: orientation of the potential ligands is optimized such that hydrophobic tails

are buried in a hydrophobic region, while the central gonane structure is surrounded by

more hydrogen bonding side-chains. The agonists identified in our preliminary screen

were docked in the EcR LDB, they interacted almost exclusively with the hydrophobic

region, which results in very favorable hydrophobic enclosure and lipophilic terms (as listed in XP descriptor analyses Table 1).

The virtual screening results predict that agonist 28 should bind most effectively to the *B. malayi* EcR LBD, however experimental EC_{50} values indicate that 37 is the most efficacious agonist, with 28 following behind in second place. Although the data set was small, a relationship was established between calculated Glide Scores and experimentally observed EC_{50}.

Conclusions

In conclusion, the data presented here demonstrates that the high throughput screening method could be applicable to screen millions of compounds rapidly with high accuracy and reproducibility. The homology model serves as another tool to validate the high throughput assay and vice versa. Both, the excellent molecular screening method and robust virtual docking study model permit rapid identification and optimization of hits for the *Bm*EcR. So far, the DAH family has not been approved for use on a large scale. But, the prospects are brighter considering the safety of these drugs [24]. After identification of the hits, the compounds could be tested on *in-vitro* culture of adult female worms, L3-stage larvae and microfilariae. The compounds that provide substantial effect on the *in-vitro* culture could be taken to a vertebrate model such as a jird. As the jird or gerbils are not natural host, the true efficacy of drugs can be tested in a natural host such as a cat or a dog. These robust models of drug discovery could aid the drug development filariasis.

Tables and Figures

Table 3.1: XP descriptor analysis given from XP docking of hormones and agonists in *B. malayi* EcR-LBD binding site.

| Compound	EC_{50} uM	Log EC_{50}	GScore	E_{Hbond}	E_{PhobEn}	$Rew_{Low MW}$	$E_{Lipophilic}$	$E_{Electro}$	$E_{Penalties}$
									XP Descriptors
20E	2.34	0.37	-7.253	-1.18	0	--	-5.263	-0.857	0.258
Muristerone A	0.05	-1.3	-8.285	-2.161	-0.565	--	-4.714	-0.869	0.168
Ponasterone A	0.04	-1.39	-9.37	-2.547	-0.677	--	-5.427	-0.747	0.233
Diacylhydrazine # 28	0.74	-0.137	-8.613	-0.574	-2	-0.277	-5.001	-0.29	0.184
Diacylhydrazine # 37	0.38	-0.42	-7.497	-0.508	-1.296	-0.278	-5.354	-0.138	0.472
Diacylhydrazine # 18	3.69	0.57	-7.374	-0.545	-0.973	-0.257	-5.3	-0.236	0.238
Diacylhydrazine # 38	0.99	-0.001	-7.269	-0.649	-0.1375	-0.438	-4.869	-0.188	0.473
Diacylhydrazine # 36	2.46	0.397	-6.587	-0.7	-0.869	-0.278	-4.654	-0.111	0.588
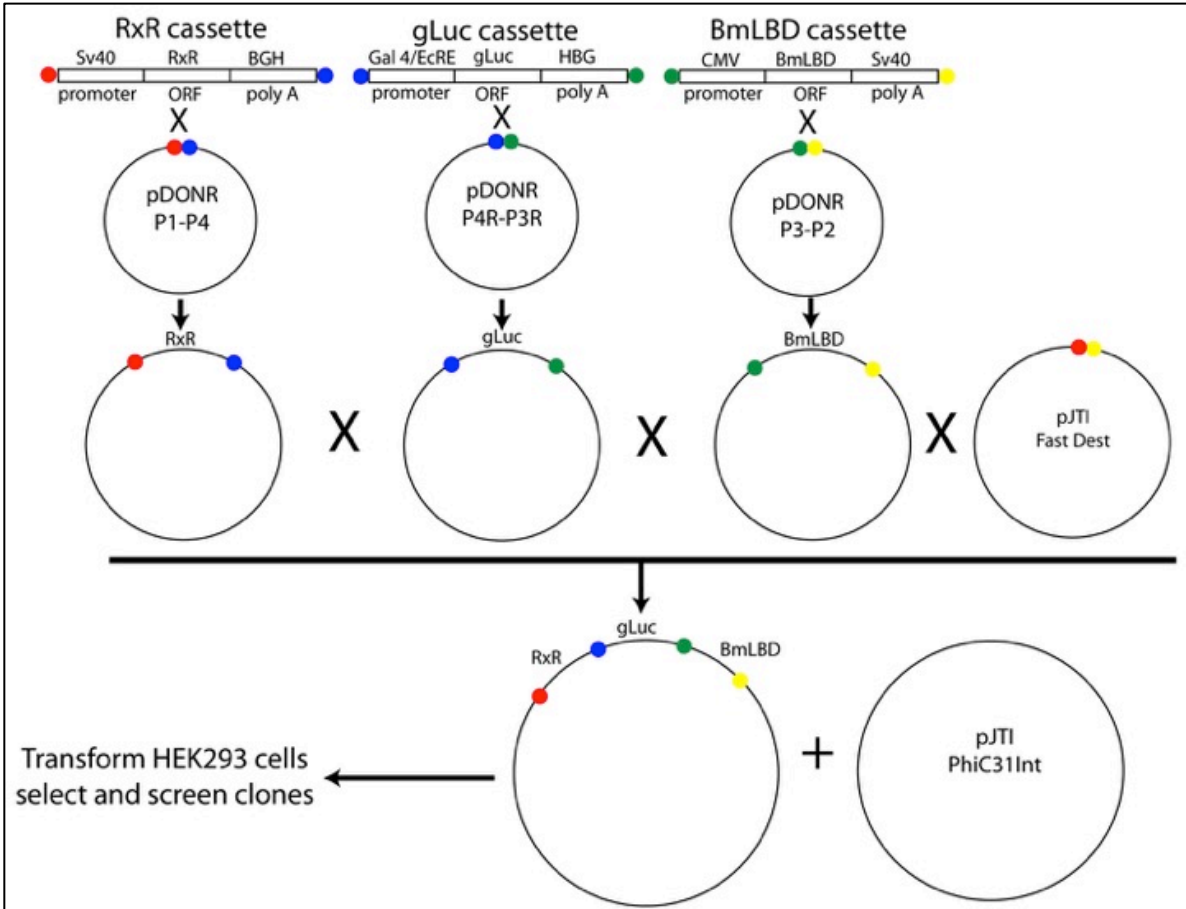
Figure 3.1: Strategy for production of a stable mammalian cell line for screening for agonists and antagonists of the *Bm*EcR. 'X" = Gateway recombination cloning. Colored circles schematically indicate the specific sequences used in the Gateway recombination cloning reactions.
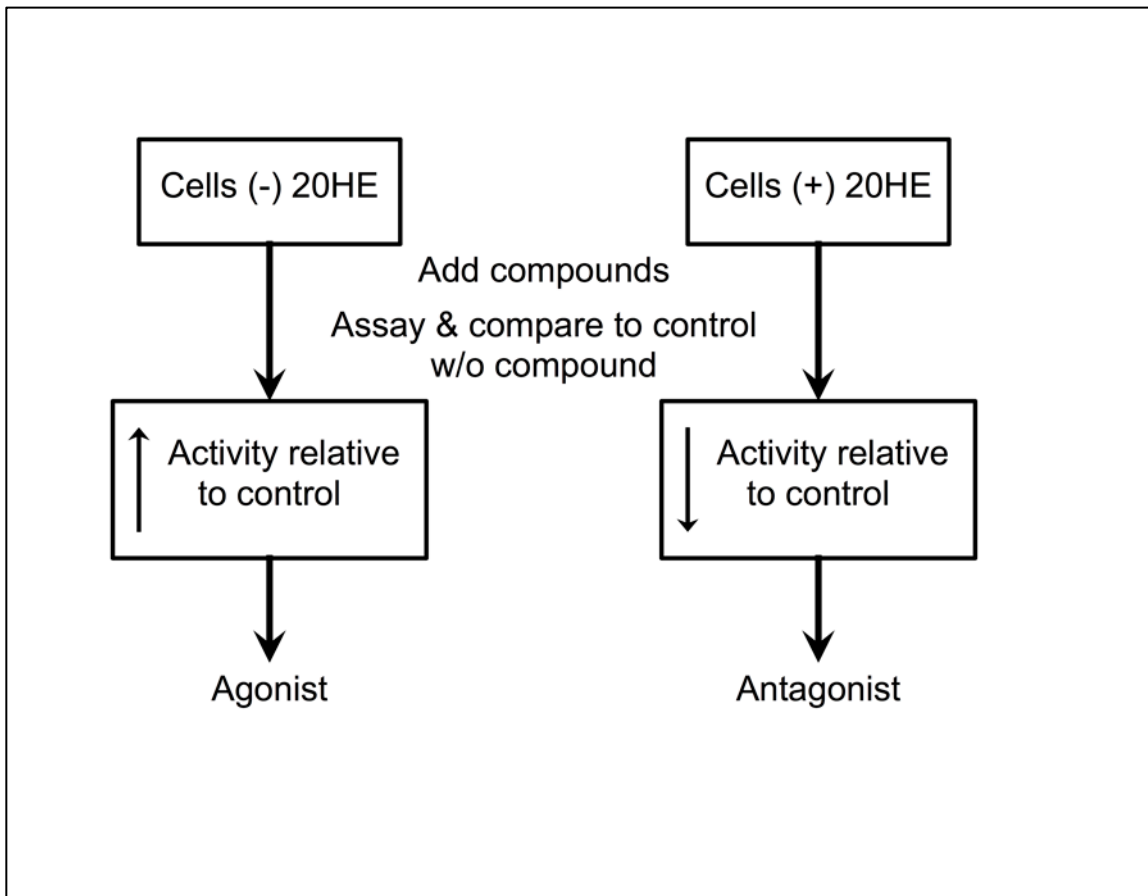
Figure 3.2: Strategy for identifying *Brugia malayi* ecdysone receptor agonists and antagonists
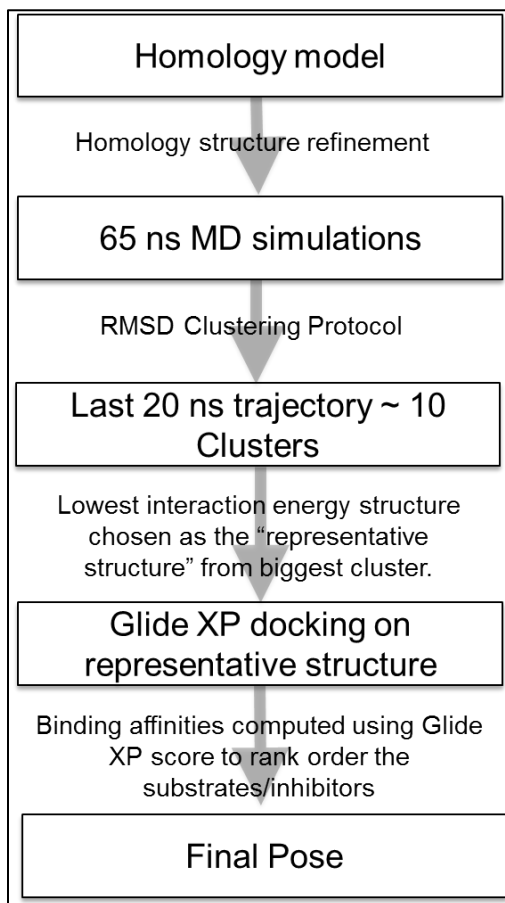
**Figure 3.3: Pipeline used to refine the homology model**
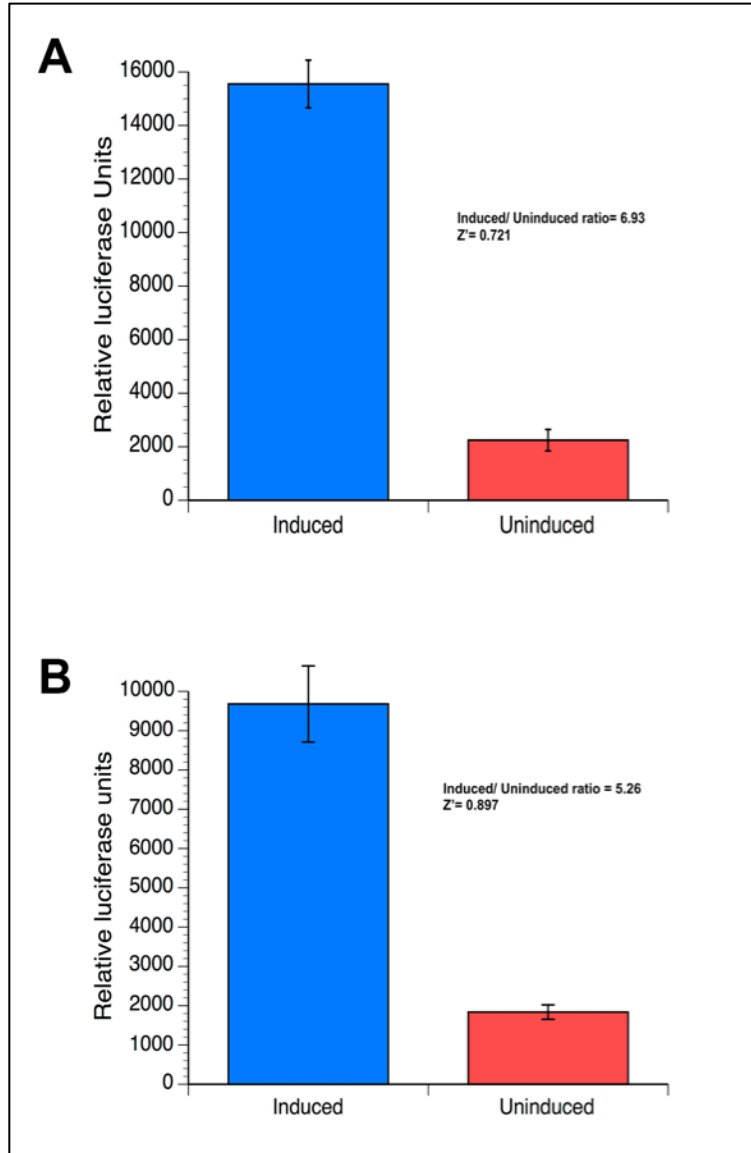
Figure 3.4: Performance of the mammalian cell assay. Results of a typical assay carried out in a 96 well format are shown. Columns indicate the mean and error bars the standard deviation of six control and six experimental wells. Assays were performed in 96 well plates. Panel A: Assay conducted with the transiently transfected cells. Panel B: Assay conducted with the stable cells.
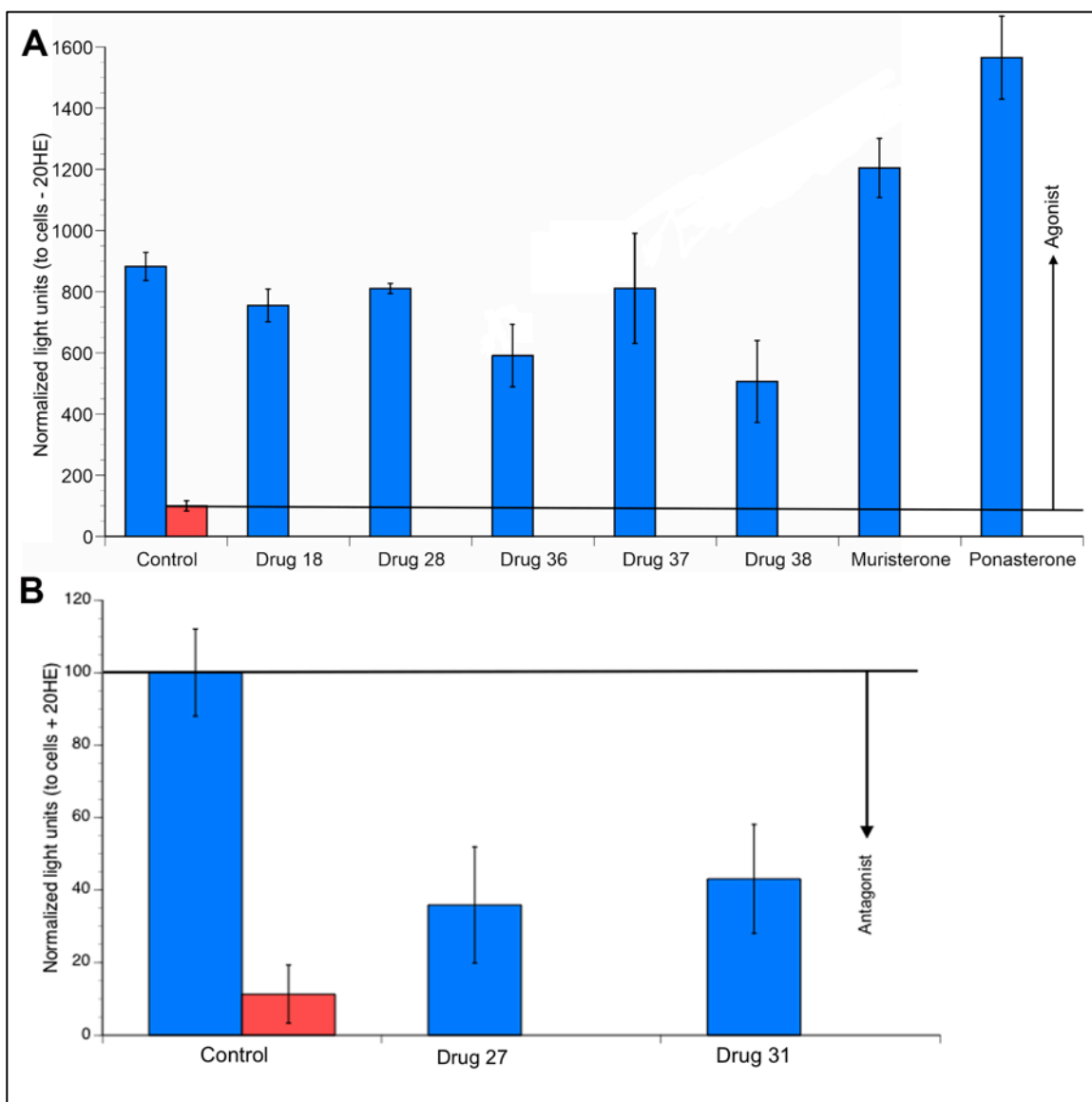
Figure 3.5: Agonists and antagonists identified in the screen of compounds active against the *Bm*EcR. Horizontal lines indicate the activity expected for compounds with no activity as agonists or antagonists. Panel A: Compounds with agonist activity. Panel B: Compounds with antagonist activity. In each panel, the columns labeled "control" represent the light units seen in cells cultured in the absence (red columns) or presence (blue columns) of 10uM 20HE. All columns represent the mean and the error bars the standard deviation in triplicate wells.

Drug ID	Structure	EC50 in uM
18		3.6872
28		0.7345
36		2.4571
37		0.3802
38		0.9959
Muristerone		0.05
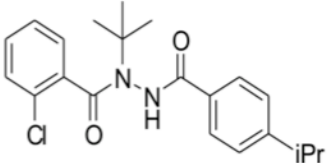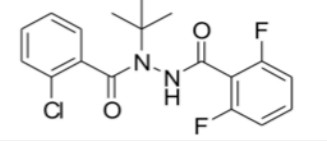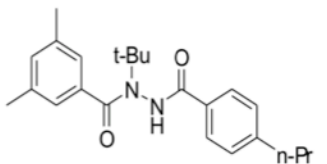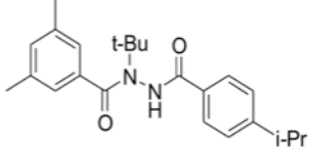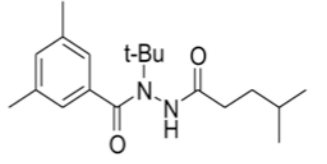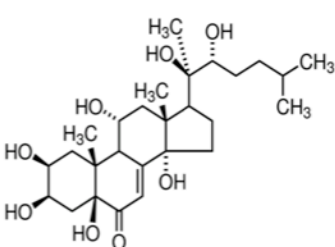
Figure 3.6: EC$_{50}$ values and structures of agonists identified in the preliminary screen of compounds interacting with the *BmEcR*.
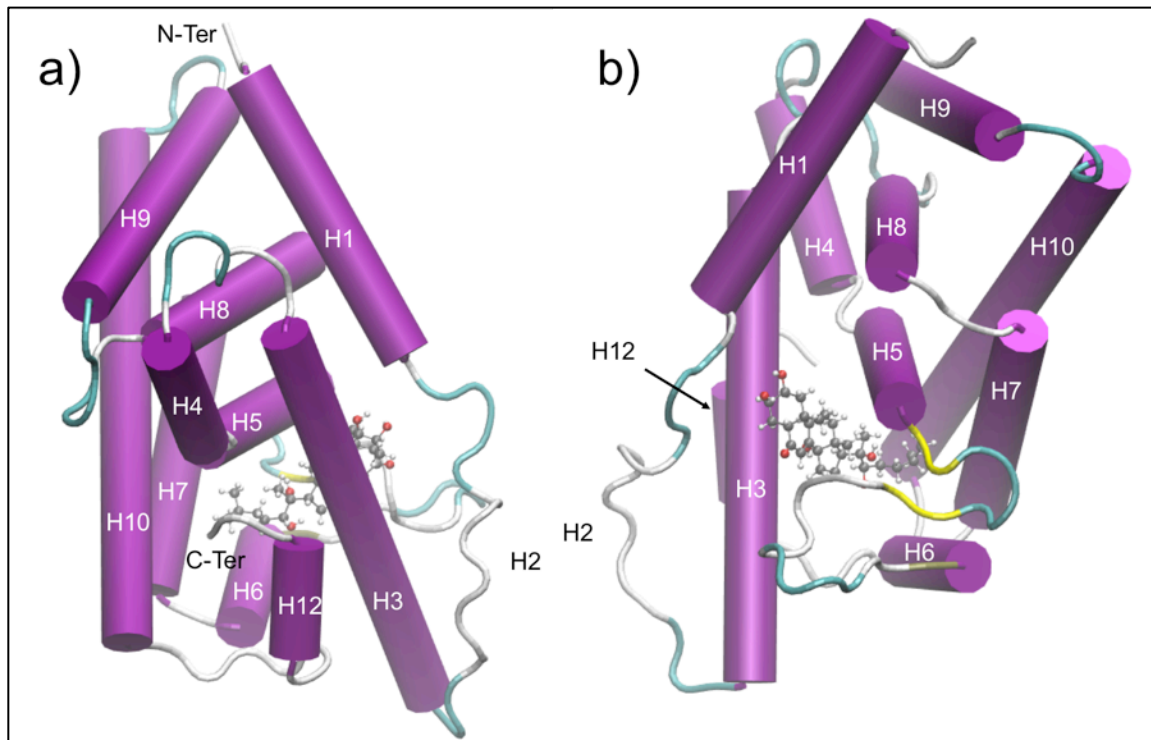
Figure 3.7: Cartoon depiction of the *B. malayi* EcR LBD homology model. The EcR is colored by secondary structural element type, with alpha-helices in purple, beta-sheets in yellow, and flexible loops in white and cyan; alpha-helices are also represented as cylinders. Ponasterone A (which was co-crystalized with the template structure) occupies the binding site with atoms colored by identity (carbon in gray, oxygen in red, hydrogen in white). The figures depict two perspectives of the same homology model: a) view with H12, DNA binding element, in the foreground, b) view with the beta-sheet and binding pocket in the foreground.
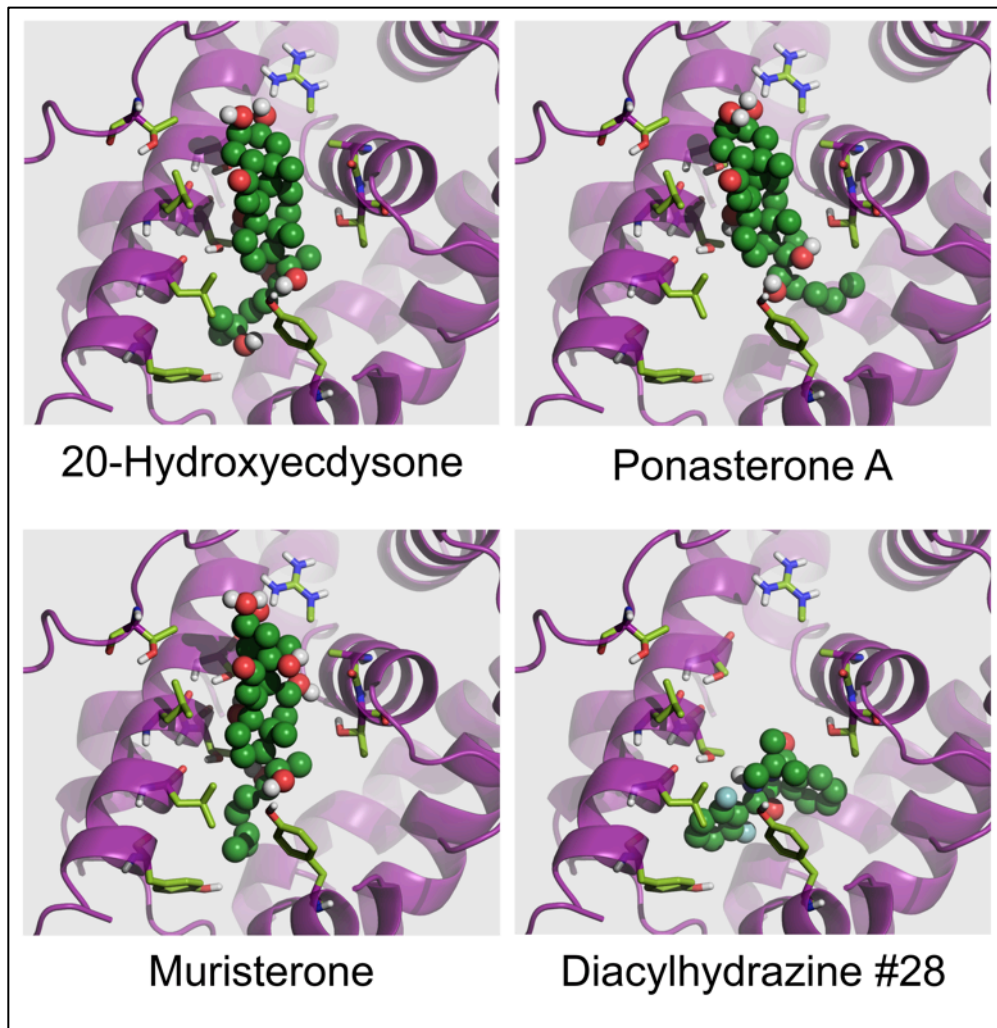
Figure 3.8: Predicted structures of agonists docking in the active site of the homology model of the *Bm*EcR LBD. The panels show 20HE, Ponasterone A, Musristerone and Diacylhydrazine #28 binding into the active site.

References

1.   Who, *Lymphatic filariasis.* 2000, World Health Organization: Geneva.

2.   Mathers, C.D., M. Ezzati, and A.D. Lopez, *Measuring the burden of neglected tropical diseases: the global burden of disease framework.* PLoS Negl Trop Dis, 2007. **1**(2): p. e114.

3.   Turner, H.C., et al., *Reaching the london declaration on neglected tropical diseases goals for onchocerciasis: an economic evaluation of increasing the frequency of ivermectin treatment in Africa.* Clin Infect Dis, 2014. **59**(7): p. 923-32.

4.   Mccarthy, J., *Is Anthelmintic Resistance a Threat to The Program to Eliminate Lymphatic Filariasis?* The American Journal of Tropical Medicine and Hygiene, 2005. **73**(2): p. 232-233.

5.   Adinarayanan, S., et al., *Diethylcarbamazine (DEC)-medicated salt for community-based control of lymphatic filariasis.* Cochrane Database Syst Rev, 2007(1): p. Cd003758.

6.   Gelband, H., *Diethylcarbamazine salt in the control of lymphatic filariasis.* Am J Trop Med Hyg, 1994. **50**(6): p. 655-62.

7.   Francis, H., K. Awadzi, and E.A. Ottesen, *The Mazzotti reaction following treatment of onchocerciasis with diethylcarbamazine: clinical severity as a function of infection intensity.* Am J Trop Med Hyg, 1985. **34**(3): p. 529-36.

8.   Awadzi, K., *Clinical picture and outcome of Serious Adverse Events in the treatment of Onchocerciasis.* Filaria J, 2003. **2**(Suppl 1): p. S6.

9.   Twum-Danso, N.A., *Serious adverse events following treatment with ivermectin for onchocerciasis control: a review of reported cases.* Filaria Journal, 2003. **2**(Suppl 1): p. S3.

10.   Tzertzinis, G., et al., *Molecular evidence for a functional ecdysone signaling system in Brugia malayi.* PLoS Negl Trop Dis, 2010. **4**(3): p. e625.

11.   Riddiford, L.M., et al., *A role for juvenile hormone in the prepupal development of Drosophila melanogaster.* Development, 2010. **137**(7): p. 1117-26.

12.   Lam, G., et al., *DHR3 is required for the prepupal-pupal transition and differentiation of adult structures during Drosophila metamorphosis.* Dev Biol, 1999. **212**(1): p. 204-16.

13. *Response Element (Molecular Biology).* [cited 2015 October 23]; Available from: http://what-when-how.com/molecular-biology/response-element-molecular-biology/.

14. Feil, R., et al., *Ligand-activated site-specific recombination in mice.* Proc Natl Acad Sci U S A, 1996. **93**(20): p. 10887-90.

15. Palli, S.R., et al., *Ecdysteroid receptors and their applications in agriculture and medicine.* Vitam Horm, 2005. **73**: p. 59-100.

16. Liu, C., et al., *Identification of genes containing ecdysone response elements in the genome of Brugia malayi.* Molecular and biochemical parasitology, 2012. **186**(1): p. 38-43.

17. Warbrick, E.V., et al., *The effect of invertebrate hormones and potential hormone inhibitors on the third larval moult of the filarial nematode, Dirofilaria immitis, in vitro.* Parasitology, 1993. **107 (Pt 4)**: p. 459-63.

18. Zhang, J.H., T.D. Chung, and K.R. Oldenburg, *A Simple Statistical Parameter for Use in Evaluation and Validation of High Throughput Screening Assays.* J Biomol Screen, 1999. **4**(2): p. 67-73.

19. Altschul, S.F., et al., *Gapped BLAST and PSI-BLAST: a new generation of protein database search programs.* Nucleic Acids Res, 1997. **25**(17): p. 3389-402.

20. Sievers, F., et al., *Fast, scalable generation of high-quality protein multiple sequence alignments using Clustal Omega.* Mol Syst Biol, 2011. **7**: p. 539.

21. Li, J., et al., *The VSGB 2.0 model: a next generation energy model for high resolution protein structure modeling.* Proteins, 2011. **79**(10): p. 2794-812.

22. Zhang, Y., *I-TASSER server for protein 3D structure prediction.* BMC Bioinformatics, 2008. **9**: p. 40.

23. Friesner, R.A., et al., *Extra Precision Glide: Docking and Scoring Incorporating a Model of Hydrophobic Enclosure for Protein-Ligand Complexes.* J. Med. Chem., 2006. **49**(Copyright (C) 2015 American Chemical Society (ACS). All Rights Reserved.): p. 6177-6196.

24. Hodgson, E., *Safer Insecticides Development and Use: Development and Use.* CRC Press.

CHAPTER FOUR

CONCLUSIONS

The EcR has been highly characterized in insects [1]. It has been used to develop compounds that can control the insect population. Targeting of the EcR in insects by the agricultural industry has proven fruitful due to the high degree of species specificity exhibited by compounds target the EcR, together with an extremely low toxicity to vertebrates [2]. Studies show that the nematodes have homolog of both the EcR and the heterodimerizing partner RXR [3, 4]. Evidence is presented portraying a functional ecdysone-signaling pathway in *Brugia malayi* [5]. But, the evidence of active system in a live parasite is unknown. The data in the first chapter suggested an active role played by the *Bm*EcR on embryogenesis. The 20HE treated adult female worms aborted high numbers of microfilariae, immature microfilariae and egg/embryos. The peak activity was reached within two days under the constant 20HE pressure in culture. The data suggests that the 20HE disrupted the reproduction developmental pathway in the worms causing precocious and premature expulsion of the life stages by the gravid adult females. The expulsion of life stages decreased by day 4 as the pressure of 20HE lead to the depletion of uterus. Although, the microfilariae appeared to be normal in the culture as compared to the microfilariae given by control untreated females, studies

need to be conducted to validate the viability and longevity of the microfilariae born

under constant 20HE pressure. Further, studies attesting the infectivity of the

microfilariae also need to be performed   The role of the ecdysone receptor on the

molting on the life stages is yet to be described. To shed a light upon this, an *in-vivo*

experiment was conducted with gerbils infected with L3 stage larva under the constant

pressure of 20HE via a subcutaneous osmotic pump. The data clearly delineates the

role played by the ecdysone receptor on molting. The parasites implanted in the

peritoneum of the treated gerbils failed to grow or molt into the next life cycle stage. As

a result no parasites were recovered from one of the animals. The one female parasite

recovered from the other treated animal clearly showed signs of growth retardation as

compared to the parasites recovered from the controls. The thin and short body of the

parasite suggests that the presence of exogenous ecdysone stimulated precocious molt

leading to stunted growth of the parasite. This study provided evidence that the

ecdysone receptor disrupted the normal molting process of the parasite.

The ecdysone pathway activates expression of a cascade of genes in insects.

These are the early and late genes controlling the molting, embryogenesis and

developmental pathways [6-8]. The genes participating in the ecdysone cascade in the

parasitic nematode *Brugia malayi* are yet to be identified. The transcriptomic analysis in

the first study identified the differentially expressed genes on stimulating the ecdysone

receptor in the adult female worm. Although very few transcripts were identified

stimulated by the pathway, the robustness of the study was depicted by the high

correlation of the duplicates samples. Majority of the genes were uncharacterized

hypothetical genes. Hence, to assess the functionality of the differentially expressed genes apart from the GO annotation, orthologs were identified using the *C.elegans* genome. Orthologs of the genes in *C.elegans* provide a good comparison of functionality over the course of evolution. The RNAi phenotypes of the *B. malayi* orthologs in *C.elegans* revealed a distinctive pattern that almost all of the genes were involved with embryogenesis. These results definitely proved involvement of the ecdysone receptor in embryogenesis and developmental pathways of the *Brugia malayi.*

More than 390 proteins were found to be more abundant in the treated worms when compared with the controls. A total of 11 genes coincided with the transcriptome and proteome. The transcriptomic and proteomic studies do not have much correlation, which may be attributed to post-transcriptional regulation of protein production, codon bias or effects on protein stability [9-14]. Despite this, the proteomic data also identified a large proportion of proteins regulating transcription. This supported the overall finding of the transcriptome analysis.

The evidence provided with the first study concluded that the ecdysone receptor is functional in the *Brugia malayi* and regulates embryogenesis and molting. It also behaves like a transcriptional factor like other nuclear receptors orchestrating expression of genes. The second study focuses on the application of the ecdysone receptor as a chemotherapeutic target. The assay based on the mammalian two-hybrid system utilized *Gaussia princeps* luciferase reporter gene along with GAL4*Bm*EcR fuion and RXR-VP16 fusion constructs. Mammalian cells transiently transfected with these

constructs give a 6-8 fold amplification of signal on addition of 10uM 20HE. The drawbacks of this assay were that all the cells do not get transfected with same efficiency and the variable transfection efficiency affected the assay performance. Although the cells give a higher fold change when transiently transfected, the assay is not easily adaptable to a high throughput format. To overcome this obstacle, a stable cell line was constructed using the constructs mentioned in chapter two. The performance of the assay with the stable cell gave a high Z' on repeated assays. This validated the use of the stable cell line for high throughput format.

The stable cell line assay was tested for reproducibility before using it to conduct the screening of the compounds. After optimization of the assay for a 96 well plate format, the assay was ready to use for high throughput screening. Several steroidal and non-steroidal ecdysone analogs were tested with the stable cell line assay. Most of the compounds belonged to the diacylhydrazine family. This class of compounds has been extensively used in agricultural industry as insecticides [15, 16]. A total of seven compounds were identified as ecdysone agonists and two as antagonists. The EC_{50} values of the compounds were in low molar and sub molar range, suggesting that they represent potentially valuable hits for further drug development. Studies need to be performed to further refine the hits by performing lead optimization. High throughput screening with thousands of synthetic and natural library of compounds could be conducted. Further, the assay should be optimized for a 384-well plate. This will dramatically increase the number of compounds tested in a high throughput format.

In order to study the ligand-receptor interaction, a homology model of the ecdysone receptor was created. Since the crystal structure of the *Bm*EcR was not available, the *B. tabaci* EcR docked with its native substrate ponesterone A was used as a template for model development. This hemipteran EcR was found to closely match the *Bm*EcR in the initial modeling exercise. The structure of the homology model was confirmed using Ramachandran plots and I-Tasser online web server. This study successfully developed a homology model for *Brugia* ecdysone receptor.

To take the homology model further, a docking study was conducted to validate the hits identified on the molecular assay. All the steroidal analogs exhibited the same conformation when docked into the active site of the *Brugia* homology model. They all interacted with almost similar residues in the active site. The non-steroidal compounds were oriented in a different pattern as of the steroidal compounds. But, they maintained the conformation taken by the diacylhydrazine family parent structure. The GlideXP scores were calculated of each docked molecule giving an estimation of the binding energy. These scores were compared with log EC_{50} value of each compound. The Pearson Correlation coefficient for the docking study and the molecular assay was quite high. This study validated the model as an *in-silico* screening tool to identify new lead compounds to bind to the *Bm*EcR.

The *in-silico* studies could be utilized to identify novel compounds binding the active site of the homology model. Virtual screening could be conducted using ZINC compounds database and PDB database to identify hits. Based on the binding scores,

the hits could be optimized structurally to bind the active site better. Structure Activity Relationship (SAR) studies could help to determine the chemical groups evoking the biological activity in the active site of the ecdysone receptor. Further, modifications of the compounds can generate novel compounds by means of substitution of a group, addition of a group or deletion of a group. Enantiomers of the compounds could also be tested virtually for the binding activity. These compounds could be custom synthesized in the medicinal chemistry laboratory and tested with the above molecular assay to generate EC_{50} and cytotoxic profile. Other libraries like focused NHR libraries, fungal extracts, ecdysone analogs library could be tested. The hits identified and optimized would to be tested in *in-vitro* and *in-vivo* model to observe performance and any side effects. The *in-vitro* models include soaking the compounds with adult female worms culture, L-3 stage larva culture and microfilarial culture. The drugs that pass the *in-vitro* testing could be taken to the animal model. The most widely used animal for the study is a gerbil. But, the gerbils are not a natural host for the *B. malayi*. The compounds can be tested for pilot *in-vivo* assays in gerbils. But, in order to gauge the true efficacy and performance of the drugs, a natural host such as a cat or a ferret would serve as a better model. The *D. immitis* dog model of the worm could also be used towards *B. malayi* as dogs can harbor natural infection. A robust pharmacological profile of the compound could be retrieved using a natural host.

The scope of this project was to develop an idea that could be aid the drug development against filariasis. Using the EcR is a rational choice as its natural absence in the vertebrates can minimize any pleotropic effects. The study validated that the

90

*Bm*EcR is playing an important role on embryogenesis and molting in the filarial worm. These are important targets for the drug development arena to combat filariasis. Additionally, drugs identified against the *Brugia* ecdysone receptor are likely to work on other filarial worms like Onchocerca volvulus without giving severe adverse reactions. With the development of an assay and homology model further aided the drug discovery process and high throughput format could screen thousands of compounds in a short span of time.

References

1.   Yund, M.A., *Ecdysteroid Action in Imaginai Discs of Drosophila Melanogaster*, in *Development of Responsiveness to Steroid Hormones*, A.M.K. Kaye, Editor. 1980, Pergamon. p. 285-302.

2.   Palli, S.R., et al., *Ecdysteroid receptors and their applications in agriculture and medicine.* Vitam Horm, 2005. **73**: p. 59-100.

3.   Palli, S.R., M.Z. Kapitskaya, and D.W. Potter, *The influence of heterodimer partner ultraspiracle/retinoid X receptor on the function of ecdysone receptor.* Febs J, 2005. **272**(23): p. 5979-90.

4.   Tzertzinis, G., et al., *Molecular evidence for a functional ecdysone signaling system in Brugia malayi.* PLoS Negl Trop Dis, 2010. **4**(3): p. e625.

5.   Liu, C., et al., *Identification of genes containing ecdysone response elements in the genome of Brugia malayi.* Molecular and biochemical parasitology, 2012. **186**(1): p. 38-43.

6.   Mansilla, A., et al., *Ligand-independent requirements of steroid receptors EcR and USP for cell survival.* Cell Death Differ, 2015.

7.   Huet, F., C. Ruiz, and G. Richards, *Sequential gene activation by ecdysone in Drosophila melanogaster: the hierarchical equivalence of early and early late genes.* Development, 1995. **121**(4): p. 1195-204.

8.   Tata, J.R., *Signalling through nuclear receptors.* Nat Rev Mol Cell Biol, 2002. **3**(9): p. 702-710.

9.   Ghazalpour, A., et al., *Comparative analysis of proteome and transcriptome variation in mouse.* PLoS Genetics, 2011. **7**(6): p. e1001393.

10.   Pascal, L.E., et al., *Correlation of mRNA and protein levels: cell type-specific gene expression of cluster designation antigens in the prostate.* BMC Genomics, 2008. **9**: p. 246.

11.   Yeung, E.S., *Genome-wide correlation between mRNA and protein in a single cell.* Angewandte Chemie (International ed. in English), 2011. **50**(3): p. 583-5.

12.   Darby, A.C., et al., *Analysis of gene expression from the Wolbachia genome of a filarial nematode supports both metabolic and defensive roles within the symbiosis.* Genome Research, 2012. **22**(12): p. 2467-77.

13.   Gustafsson, C., S. Govindarajan, and J. Minshull, *Codon bias and heterologous protein expression.* Trends in biotechnology, 2004. **22**(7): p. 346-53.

14. Greenbaum, D., et al., *Comparing protein abundance and mRNA expression levels on a genomic scale.* Genome biology, 2003. **4**(9): p. 117.

15. Yoshio Takei, H.A., Kazuyoshi Tsutsui, *Handbook of Hormones: Comparative Endocrinology for Basic and Clinical Research*. 2015: Elsevier Science & Technology 674.

16. Feil, R., et al., *Ligand-activated site-specific recombination in mice.* Proc Natl Acad Sci U S A, 1996. **93**(20): p. 10887-90.

APPENDICES

Appendix for Chapter One

Table S1: Primers and probes used for the real time PCR

Amplicon Size (bp)	Gene		Primer
104	*Bm*58	Forward Reverse Probe	5' ACGAGCAACAGGACTTGT 3' 5' AACGACCACCTTCAGGT 3' 5' FAM- TCACTTGTACATCGCTATTTAACTGGTGCT - BHQ1 3'
83	*Bm*12555	Forward Reverse Probe	5' CTTTCGTAGAACGGTTCGTG 3' 5' CGTTACGACCAGCTTTATCAA 3' 5' FAM-ACGTGTGTCGTTATGAGCAGAAGTGT- BHQ1 3'
103	*Bm*11454	Forward Reverse Probe	5' GTGGAGGATACGGTTATGGTAAA 3' 5' CTGATAGCAATATCATACCCTCTATAT 3' 5' FAM-AAATTGCCGAGATGGGTGCCTACG-BHQ1 3'
123	*Bm*7925	Forward Reverse Probe	5' GAACCAGAAACGCTGAAAGTG 3' 5' CCGATATGATGGTCGTCGATT 3' 5' FAM-AATCAGTGACGATGAGGCACGA-BHQ1 3'
105	*Bm*2121 (NADH)	Forward Reverse Probe	5' GCTTATAAAGCTGGATTTATTGGC 3' 5' TGTTTCTTCACCACATATATAGGC 3' 5' HEX-ACGTATTCGTTCATCGAGGTGCTGG- BHQ1 3'

Appendix for Chapter Two

Homology model construction and validation

In order to validate the EcR homology model, PROCHECK was used to compile a Ramachandran plot, or plotted distribution of the backbone (φ,ψ) dihedrals[1]. PROCHECK validates that our homology model has backbone dihedral distribution very similar to that of "natural" protein structures with 89.6 % of (φ,ψ) pairs present in the most favored regions. To verify the reproducibility of our homology model, we used the online homology modeling web-server I-TASSER [2], to create a second homology model using third party procedures for comparison purposes. The Figure SI-1 summarizes the pipeline used to create the homology model. Our homology model retained the same secondary and tertiary structures in comparison with the top ranked I-TASSER homology model. The Figure SI-2 shows the superposition of Prime homology model over I-Tasser homology model.

A Ramachandaran plot was compiled to compare the distribution of backbone dihedrals (phi-psi) of our EcR homology model to the known distributions of these dihedrals amongst all crystallized proteins in the Protein Data Bank. 89.6% of all amino acids in our homology model had phi-psi dihedral pairs plotted within "favored" regions of backbone conformations, i.e., regions that are highly populated by amino-acids in "nature-made" polypeptides. This result supports that our constructed homology model is very similar to most described proteins with regards to backbone orientation which relates to minimization of backbone strain.

Ecdysone receptors from *Bemisa tabaci* and *Heliothis vericens* insect species have been crystalized and described. As proteins with the same functions as, and closely related to the *B. malayi* EcR, these structures will serve as guides to scrutinizing the predicted teriary elements of our *B. malayi* EcR homology model. Our model exhibits 10 of the 11 expected α-helices and the one expected β-sheet comprised of three strands, when compared to *B. tabaci* and *H. vericens* EcR crystal structures. The model also exhibits the same general fold common to the EcR family: 11 to 12 alpha helices arranged antiparallel with respect to their neighbors and stacked in three "layers" with one beta-sheet encompassing one side of the binding pocket. Additionally, our homology modeling protocol was able to predict the placement of α-helix-12 (H12), a secondary structural element that is crucial to the function of the EcR.

The online wed-server, I-TASSER, which constructs homology models from submitted sequences, was used to construct a second homology model of the *Bm*EcR-LBD to compare to our model constructed with Schrodinger's Prime module. As is shown in Figure SI-3, our model and the I-TASSER generated model agree on placement of secondary structural elements and the overall EcR fold is present in both. Furthermore, the two structures agree on placement of residues within the binding site.

Homology model refinement

To refine the homology model further, by allowing it to access more relaxed conformations, and to ensure the model was stable, it was simulated with molecular dynamics (MD) simulations in CHARMM (Chemistry at HARvard Molecular Modeling)

the biomolecular simulation program[3], CHARMMing [4] and pdbtools (https://github.com/JoaoRodrigues/pdb-tools) were used to convert the homology model to a CHARMM compatible version and to generate necessary topology and coordinate files. The protein was treated with CHARMM (C36) force-fields and parameters for substrate ponesterone A were generated using the CHARMM generalized force-field (CGenFF) via the Paramchem Web-interface [5]. A total of 76,128 TIP3 water molecules were added to solvate the homology model, and waters that overlapped with protein atoms were deleted. The resulting system was a cubic box of 80 x 80 x 80 Å with the EcR model at the center. Next, the system was neutralized by adding sodium and chlorine ions sequentially, replacing random water molecules, until the total salt concentration was 0.15 M NaCl. This neutralization step was followed by short (10 steps) of steepest descent (SD) minimization and then 25 steps of *Adopted Basis Newton-Raphson* (*ABNR*) minimization to alleviate steric clashes that may have arisen during the ion placement. Slowly the system was heated from 100 K to 300 K for 100 ps and after heating the system was equilibrated and simulated for a period of 65 ns under isobaric-isothermal conditions (*NPT ensemble). A* 2 fs integration time step was used, and snapshots were saved for every 1000 steps (2 ps). The SHAKE algorithm constrained covalent bonds to hydrogen atoms. Particle mesh Ewald (PME) was used for evaluating long-range electrostatics and a 12Å cut-off was used to calculate LJ-nonbonded terms. *To improve computational speed, the 65ns simulation was conducted with GPU accelerate code and the* CHARMM/OpenMM interface[6]. To monitor the structural stability and convergence of the homology model across the trajectory, structural properties like radius of gyration (R_g), root mean square deviation (RMSD),

root mean square fluctuation (RMSF) and total energy of the system were reported. These time correlated properties are shown in Figure 4 a,b,c. Additionally, root mean square fluctuation (RMSF) was calculated for each residue (using the complete 65ns trajectory) to estimate which regions of the EcR model are most or least flexible. RMSD and R_g plots support that the model was equilibrated within the first 20 ns of simulation. Total energy also remains stable, fluctuating steadily around ~ -140500 kcal/mol; with no large total energy drifting indicated in Figure SI-4c, it is apparent that the simulation is converged. RMSFs are given in Figure SI-4d and Table SI-1 for those residues within 3Å of the hormone binding site. As most residues presented in Table SI-1 below exhibit RMSFs of < 2Å, binding site residues are relatively inflexible during MD simulations.

Virtual Screening Studies:

In order to obtain a single snapshot that represented the equilibrated portion of the 65 ns trajectory, all frames from the last 20 ns were clustered according to an RMSD cut-off in CHARMM's CORREL module, this resulted in 10 unique clusters. Then, the interaction energy between ponasterone A and the protein system was calculated for each frame in the highest populated cluster. The frame with the lowest (most favorable) interaction energy was chosen as the representative structure of *B. malayi*'s EcR, and this structure was used as the binding site during docking studies. The lowest energy pose (as predicted by Glide Score) of **20-hydroxyecdysone** bound in *B. malayi* EcR predicts the hormone's hydrophobic tail to be supported via van der Waals interactions to several residues including Leu44, Ile120, Phe119, Tyr41, Ile222, and Ile220. However, the central gonane structure of 20-hydroxecdysone, is surrounded

by residues in the binding pocket of similar character to itself including Thr89, Thr48, Tyr116 as well as some hydrophobic residues, Leu47, Leu85, and Val100. GlideXP docking also predicts on the other side of the binding pocket, Arg88's NH_2 will donate a hydrogen bond to C_3-OH of 20-hydroxecdysone. **Ecdysone** is also predicted to bind in the EcR LBD binding pocket such that the hydrophobic tail can interact with a collection of mostly hydrophobic residues -- including Ile120, Tyr116, Tyr41, and Leu85 -- while C_{25}-OH of the tail accepts a hydrogen bond within this hydrophobic pocket from Tyr41-OH. Additionally, as also seen with 20-hydroxyecdysone, ecdysone's C_3-OH accepts a hydrogen bond from Arg88-NH_2. **Muristerone A** is oriented similarly to 20-hydroxyecdysone and ecdysone in the EcR LBD binding pocket with the hydrophobic tail interacting heavily via van der Waal and hydrophobic contacts to Ile120, Phe119, Tyr41, and Leu44. Muristerone A's C_3-OH also participates in hydrogen bonding, this time donating a hydrogen bond to Thr22-OH. **Ponasterone A** is also oriented in the binding site with the hydrophobic tail interacting with the grouped hydrophobic residues on one side, and the more polar end of the molecule interacting via hydrogen bonding. Leu85, Leu120, Phe128, and Met127 interact via van der Waals contacts with the tail and similar to 20-hydroxyecdysone and ecdysone, Arg88-NH_2 donates a hydrogen bond to C_3-OH of ponasterone A.

Out of all agonists, compound 28 has the lowest Glide Score. **Compound "28"** is predicted to bind in the hydrophobic region of the binding pocket; out of the 17 residues within 5Å of compound 28, 16 are hydrophobic (within 3Å of 28: Ile120, Met127, Thr48, Leu85, Leu44, Val100, and Tyr116, within 5Å of 28: Leu47, Phe128,

99

Leu123, Ile222, Tyr41, Phe119, Val86, Ile215, Ile220, Ala131, Leu102). GlideXP predicts compound 28, with two aromatic rings, participates in aromatic interactions to Tyr41 and Tyr116, both of parallel displaced style aromatic interaction. Additionally, much of the binding energy should be attributed to van der Waals interactions between alkyl substituents on the ligand and hydrophobic residues in the binding site including Val100, Met 127, Leu85, and Leu44. The Glide docking score Table 3.1 predicts compound 28 binds most favorably out of six agonists with GScore of -8.613, and this is largely due to the highly favorable hydrophobic enclosure term of -2.000 and the lipophilic term of -5.001.

Like 28, **Compound "34"**, is too predicted to bind in the hydrophobic pocket and interact mostly via van der Waals terms to Ile120, Met127, and Tyr116. However, binding of 34 is unique as it exhibits electrostatic interactions between charged Arg88 side chain and the three fluorines of compound 34. Additionally, 34 donates a hydrogen bond to Thr89OH. Compound 34 has a GScore of -8.132, which is composed most notably of the hydrophobic enclosure term (-1.575), the Hbond term (-0.700), the lipophilic term (-5.289), and the electrostatic term (-0.400). This electrostatic contribution is the most favorable electrostatic contribution seen amongst all six agonists, and is likely a result of the interaction between Arg88 and fluorine atoms.

Compound "37" binds in the hydrophobic binding pocket and is supported by van der Waals interactions to Ile120, Phe128, Ala124, Tyr116, and Leu85. Compound 37 also donates a weak (as the angle is not optimal) hydrogen bond to Thr89-OH. The

calculated GScore for 37 is -7.497, with largest contributing terms again being the hydrophobic enclosure (-1.296) and the lipophilic term (-5.354).

Compound "18" is predicted to also bind in the hydrophobic pocket and interact mostly via van der Waals terms to Ile120, Leu102, Leu44, Ile222, and Ile215. Compound 18 is also predicted, like 28, to form parallel-displaced aromatic interactions to Tyr116 and to Phe128. The calculated GScore is -7.374 for 18, with the highest contributions again from the hydrophobic enclosure term (-0.973) and the lipophilic term (-5.3).

Compound "38" binds in the hydrophobic pocket and interacts via van der Waals terms to Tyr116, Ile120, Ile120, Leu44, Phe128, and Leu47. Additionally, Tyr116 forms a parallel-displaced aromatic interaction to compound 38's aromatic ring and Thr48 accepts a hydrogen bond from compound 38's-NH. Compound 38 has a GScore of -7.269, and again with the most prominent terms being the hydrophobic enclosure term (-0.649) and the lipophilic term (-4.869).

Finally **Compound "36"** binds in the hydrophobic binding pocket, and similarly interacts with Leu102, Val100, Phe128, Leu85, Ile120, and Ala124 via van der Waals contacts. GlideXP also predicts compound 36 will donate a hydrogen bond, from a nitrogen hydrogen, to Thr89-OH. Compound 36 has a GScore of -6.587 with the hydrophobic enclosure term contributing -0.700 and the lipophilic term contributing -4.654.

Tables and Figures

Table SI-1: Summary of RMSFs calculated from the MD simulation of for all residues within 3 Å of the 20-hydroxyecdysone binding site. Residue name is given on the left of each column and the RMSF is given to on the right, residues are ordered by their residue number. Polar residues are highlighted in blue, hydrophobic residues are listed in black and those residues constituting the "hydrophobic pocket" are underlined.

Residue	RMSF(Å)		Residue	RMSF(Å)		Residue	RMSF(Å)		Residue	RMSF(Å)
Thr25	*4.0197*		Leu54	1.0319		Gly103	1.0891		Ala124	1.5249
Tyr41	1.4307		Leu85	1.0164		Leu102	1.2015		Met127	1.8614
Leu44	1.4337		Arg88	1.0116		Tyr116	1.5545		Phe128	1.6413
Leu47	0.9546		Thr89	0.8653		Phe119	*2.1285*		Ile220	*2.2800*
Thr48	0.8501		Cys92	1.2423		Ile120	1.8953		Ile222	*2.7519*
Ser51	0.6974		Val100	1.1788		Ile123	*2.4866*			

Table SI-2: Summary of the phi-psi distribution for amino acids in the EcR-LBD homology model. The sum of the first two percentages indicates the number of residues in more favored regions (98.7%).

Number of residues in favored regions	90.5%
Number of residues in allowed regions	8.2%
Number of residues in outlier region	1.3%
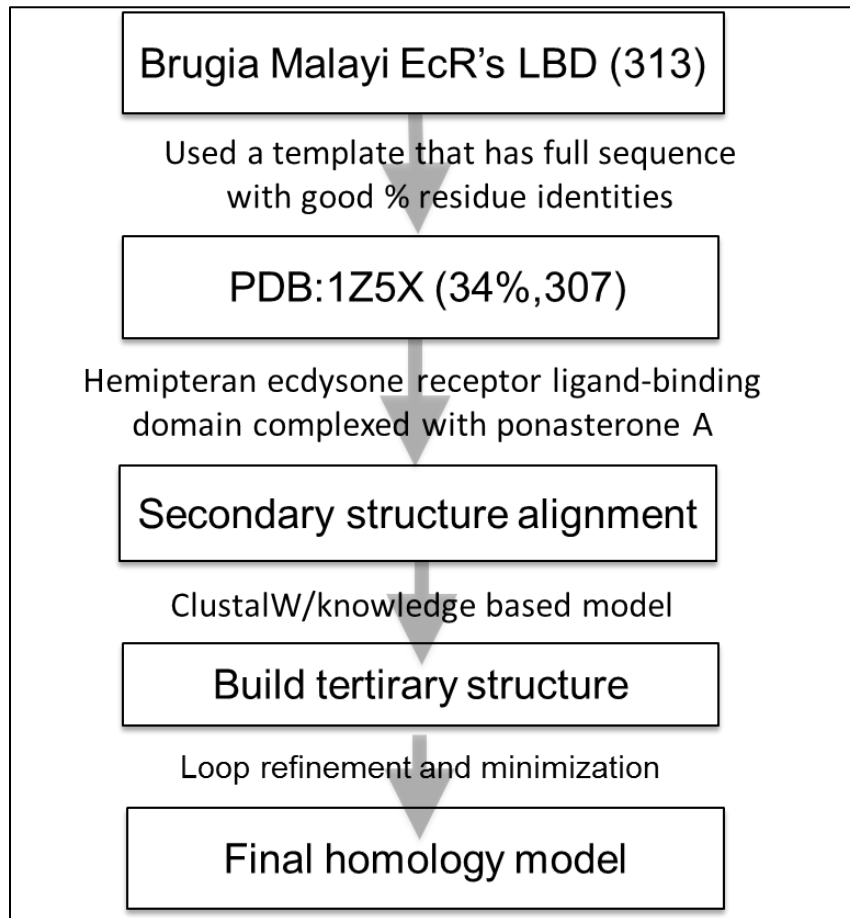
**Figure SI- 1: Pipeline to create homology model**
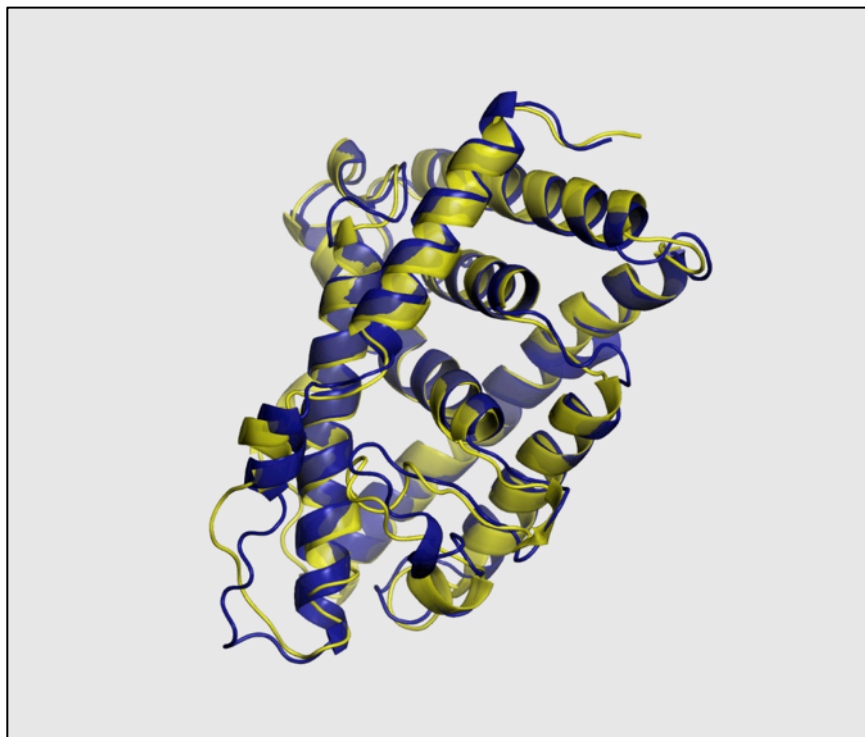
Figure SI-2: Superposition of Prime homology model(yellow) over I-Tasser homology model (blue).
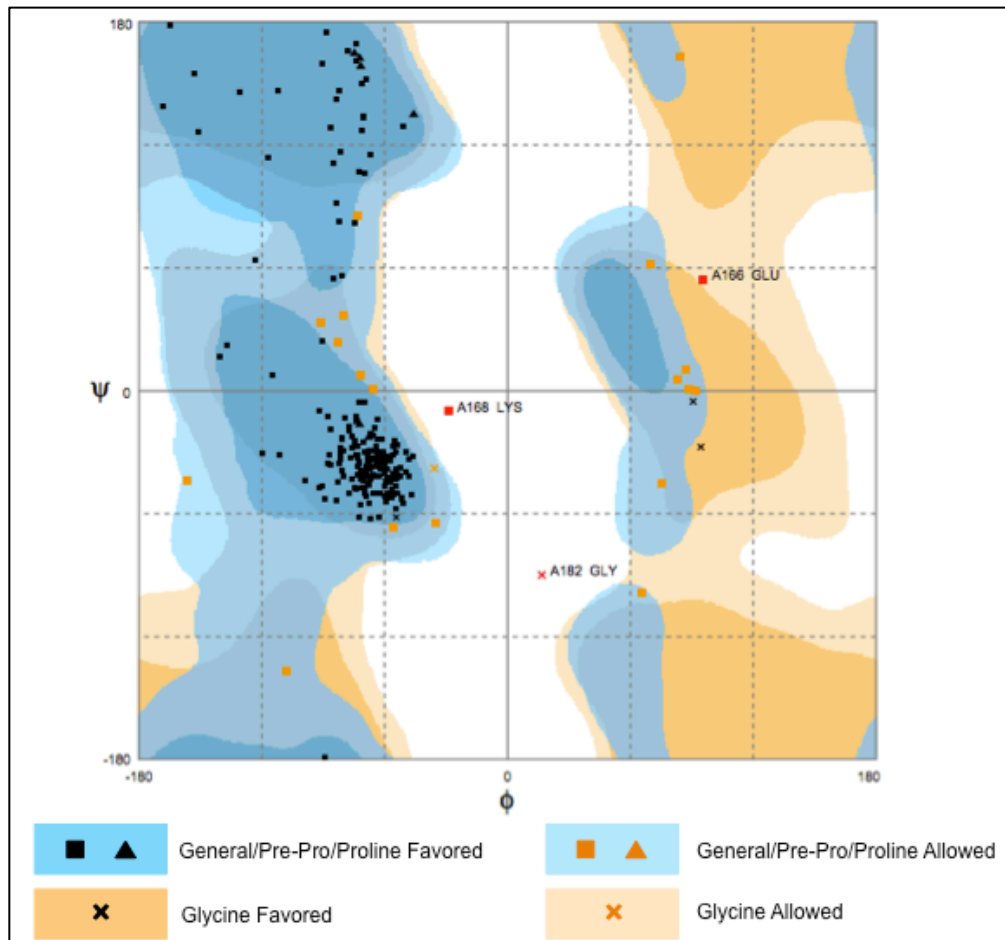
Figure SI-3: Ramachandaran plot compiled of the phi-psi backbone dihedrals from the model after molecular dynamics simulations. The legend illustrates the color designations of certain regions in the plot.
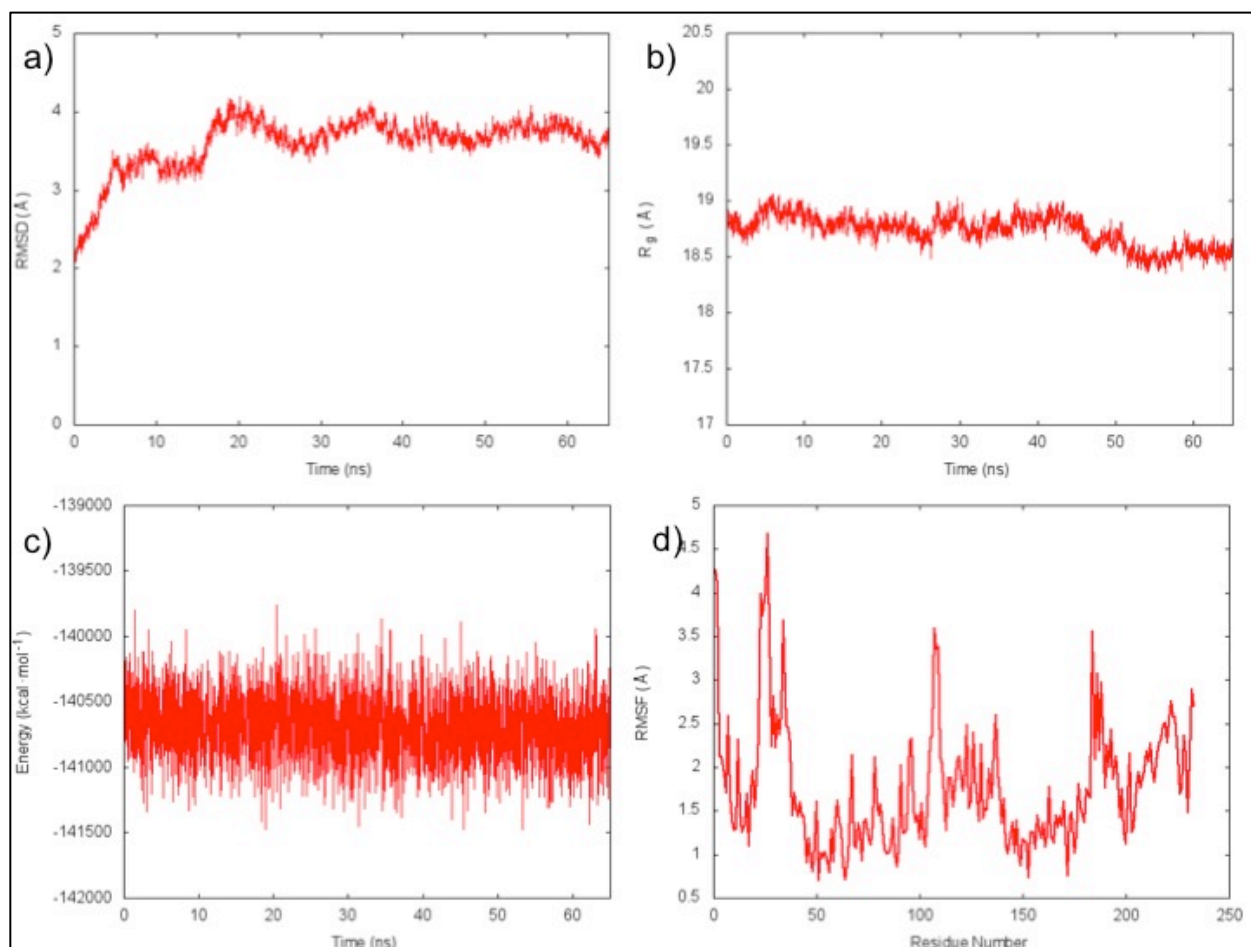
Figure SI-4: MD simulation results: a) RMSD plotted over the course of 65 ns simulation, b) radius of gyration plotted over the course of 65 ns simulation, c) total energy of the homology model and ponasterone A complex monitored over the course of 65 ns simulation, and d) RMSF analysis for each residue in the EcR LBD homology model.

References

1. Laskowski, R.A., et al., *PROCHECK: a program to check the stereochemical quality of protein structures.* Journal of Applied Crystallography, 1993. **26**(2): p. 283-291.

2. Zhang, Y., *I-TASSER server for protein 3D structure prediction.* BMC Bioinformatics, 2008. **9**: p. 40.

3. Brooks, B.R., et al., *CHARMM: The biomolecular simulation program.* Journal of Computational Chemistry, 2009. **30**(10): p. 1545-1614.

4. Miller, B.T., et al., *CHARMMing: a new, flexible web portal for CHARMM.* Journal of Applied Crystallography, 2008. **48**(9): p. 1920-9.

5. Vanommeslaeghe, K., et al., *CHARMM General Force Field (CGenFF): A force field for drug-like molecules compatible with the CHARMM all-atom additive biological force fields.* Journal of computational chemistry, 2010. **31**(4): p. 671-690.

6. Hynninen, A.P. and M.F. Crowley, *New faster CHARMM molecular dynamics engine.* Journal of Computational Chemistry, 2014. **35**(5): p. 406-13.